MOUNTAIN-PLAINS CONSORTIUM

MPC 19-378 | K. Ng, D. Mebrahtom, and K. Ksaibati

Characterization of Crushed Base Materials in Wyoming

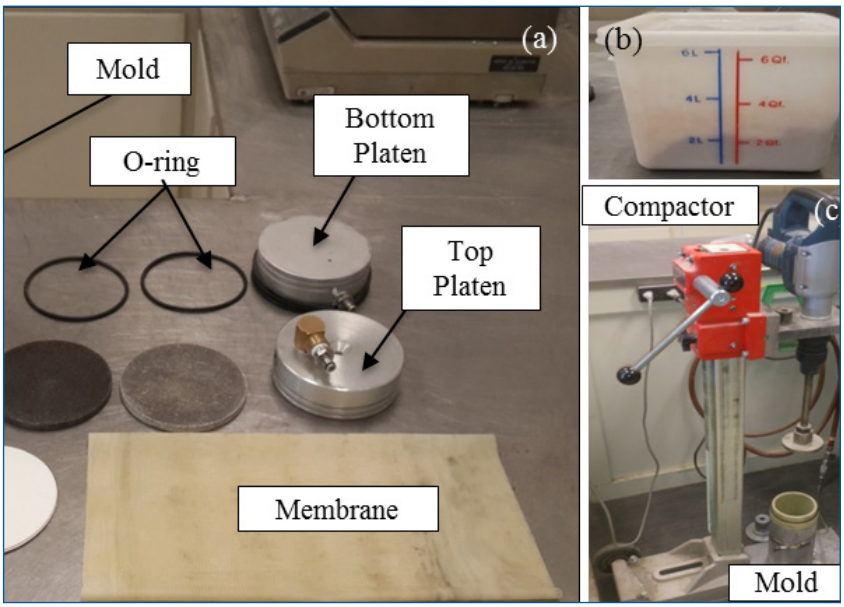

MOUNTAIN-PLAINS CONSORTIUM REGION 8

A University Transportation Center sponsored by the U.S. Department of Transportation serving the Mountain-Plains Region. Consortium members:

Colorado State University
North Dakota State University
South Dakota State University
University of Colorado Denver
University of Denver
University of Utah
Utah State University
University of Wyoming

Characterization of Crushed Base Materials in Wyoming

Prepared by:

Kam Ng, Ph.D., P.E., Associate Professor
Dawit Mebrahtom, Graduate Assistant
Khaled Ksaibati, Ph.D., P.E., Professor

Department of Civil & Architectural Engineering
University of Wyoming
1000 E. University Avenue, Dept. 3295
Laramie, Wyoming 82071

March 2019

Acknowledgements

The authors would like to thank the Mountain Plains Consortium (MPC), Wyoming Department of Transportation (WYDOT), and the Federal Highway Administration (FHWA) for funding this research project. The authors would like to specially thank the following people contributing to this project: Ryan Steinbrenner, Mike Farrar, Greg Milburn, Bob Rothwell, Mano Martinez, Kurtis Briggs, Cory Rinehart, and Dr. Shaun Wulff. Also, special thanks to Mr. Timothy McDowell and Ms. Enid White from the WYDOT Research Center, and the WYDOT research advisory committee members for supporting this research project.

Disclaimer

The contents of this report reflect the views of the authors, who are responsible for the facts and the accuracy of the information presented. This document is disseminated under the sponsorship of the Department of Transportation, University Transportation Centers Program, in the interest of information exchange. The U.S. Government assumes no liability for the contents or use thereof.

ABSTRACT

To improve the pavement design and construction in Wyoming, the Wyoming Department of Transportation (WYDOT) is adopting the Mechanistic-Empirical Pavement Design Guide (MEPDG). A full implementation of MEPDG requires the characterization of local crushed base materials. In this research, laboratory experiments on resilient modulus were performed to characterize the local crushed base materials in Wyoming. A comprehensive resilient modulus test program was completed by following the WYDOT modified AASHTO T 307, which incorporates WYDOT design and testing practices. The cyclic triaxial testing chamber for confining load application, two axial load sensors, and two spring-loaded linear variable transducers (LVDTs) to measure the recoverable axial strain of an aggregate specimen were used in determining the laboratory resilient modulus. Effects of moisture content, percent fine, stress, gradation, and fractured face on base resilient modulus were assessed, and estimation models were developed using statistical methods. The coefficients of constitutive models developed by NCHRP (2004) and Hicks and Monismith (1971) were calibrated for the locally available crushed base materials. Finally, a design table and chart for the estimation of base resilient modulus was developed to facilitate the full implementation of the MEPDG in Wyoming.

TABLE OF CONTENTS

LIST OF FIGURES

LIST OF TABLES

1. INTRODUCTION

1.1 Background

The design of proper and cost effective pavement structure requires input of different variables and interactions that could affect pavement performance. This requirement is set out in the Mechanistic-Empirical Pavement Design Guide (MEPDG), initiated by the National Corporative Highway Research Program (NCHRP). The MEPDG guide eliminates the limitations of the American Association of State Highway and Transportation Officials (AASHTO) Guide for Design of Pavement Structures (1993), which requires laboratory determined pavement material inputs, local climate inputs, performance criteria inputs, design reliability inputs, and traffic inputs. Resilient modulus of a pavement layer is one of the major factors affecting the pavement responses to the applied load. Resilient modulus is also one of the main input variables to the MEPDG software.

In an effort to implement MEPDG in Wyoming, determination of the resilient modulus of the intermediate layer or base layer complements the recently completed research on subgrades by Hellrung (2015), Henrichs (2015), and Ng et al. (2017).

1.2 Problem Statement

Wyoming Department of Transportation (WYDOT) is moving toward a full implementation of the MEPDG by determining the pavement layer moduli. At this stage, a design catalog of aggregate base properties is not available. The design catalog developed from this study summarizes the material inputs so that limitations can be eliminated, and pavement performance can be improved to ultimately allow for a cost-effective pavement design in Wyoming. The primary aim of this research project was to locally calibrate the properties of base materials in order to reduce model errors and improve prediction accuracy.

A research project to determine the resilient modulus of the subgrade layer in Wyoming was recently completed (Ng et al., 2017). In that research project, the resilient modulus of base layers was estimated using a falling weight deflectometer (FWD) while the resilient modulus of the subgrade layer was measured using a laboratory test method and FWD. The estimated base layer modulus was used in the FWD method for the back-calculation of the subgrade moduli. This lead to extreme differences in resilient modulus values between the base and subgrade materials with subgrades having higher resilient modulus values. An effort to combat the differences in base and subgrade, back-calculation of modulus value was done using a fixed base layer approach. However, there was no measured base modulus for comparative studies, preventing the realistic characterization of the base properties and limiting the implementation of MEPDG in Wyoming. Using this research as a guide, it can be inferred that characterization of the local base materials will facilitate the use of MEPDG software in the design of flexible and rigid pavements.

1.3 Objectives

This research project included the following objectives:

1. Characterize the properties of local base materials.
2. Understand effects of rock type, moisture content, percent fine and gradation on base resilient modulus.
3. Improve the base modulus estimation.
4. Facilitate the comprehensive implementation of MEPDG in Wyoming.

1.4 Research Tasks

The following research tasks were completed to accomplish the research objectives:

1.4.1 Task 1: Literature Review

This task focused on a literature review related to base resilient modulus testing and significant factors affecting the resilient modulus. The review included 1) summary of current knowledge and practice in the characterization and estimation of base properties to be used for the implementation of MEPDG in Wyoming; 2) current specifications and guidelines pertinent to the base material inputs prepared by Departments of Transportation (DOTs) and national agencies, such as AASHTO and Federal Highway Administration (FHWA); and 3) any related analytical and experimental studies to provide information for potential adaptation and application in Wyoming.

1.4.2 Task 2: Identify Base Materials and Determine Standard Properties

This task focused on identifying the base materials sources throughout Wyoming from the past or current road projects for standard aggregate testing and the subsequent resilient modulus experiment described in Task 3. The process of identifying tested materials and determining the standard properties was done in conjunction with WYDOT Materials & Testing Program. The study compiled standard base properties include classification, gradation, density-moisture relationship in accordance with the AASHTO T-99 (2010), and R-value determined in accordance with the ASTM D2844 (2007). These properties were also used for subsequent data analysis and correlation studies in Task 4.

1.4.3 Task 3: Resilient Modulus Experiment

This task focused on conducting the resilient modulus experiments on the base materials identified in Task 2. The prepared specimens were compacted following the WYDOT modified AASHTO T 307 developed by Henrichs (2015). The base materials were prepared at four different moisture contents. The experiment was conducted following the preconditioning and 15 test sequences described in the WYDOT modified AASHTO T 307 using the cyclic tri-axial testing equipment at WYDOT Materials and Testing Program. After completing the resilient modulus cyclic tri-axial test, all base materials that attained less than 5 percent total permanent deformation were subjected to static triaxial loading with a 5-psi confining pressure referred as the quick shear test.

1.4.4 Task 4: Data Analysis and Correlation Study

This task focused on analysis of data obtained in Task 3. The measured resilient modulus values were plotted as a function of deviator and confining stresses for each material. The effects of rock type, R-value, percent fines, and modified proctor density and moisture content were examined. The measured standard test results and resilient modulus values were compared to produce the following deliverables:

- Develop a catalog of standard properties including a design table and a design chart of resilient modulus values for the base materials.
- Calibrate stress-dependent constitutive models in terms of the three-regression coefficients (K_1, K_2 and K_3) using the measured resilient modulus values through linear and non-linear regression analyses.
- Establish empirical relationships between standard test properties and resilient modulus using multiple regression analysis techniques.

1.5 Outcomes

The research findings provide WYDOT, as well as other transportation agencies nationwide, the necessary models to estimate resilient modulus of granular crushed base materials. The locally calibrated resilient modulus of base materials and aforementioned deliverables will enhance the pavement design efficiency and facilitate the full implementation of MEPDG in Wyoming.

1.6 Report Organization

This report consists of five sections, which are briefly described below. References are included following Section Five.

- *Section One* introduces the project tasks and research objectives accomplished by research team. In this section, the research outcomes are also summarized.
- *Section Two* summarizes a literature review of past and present research related to characterization of base materials. Factors affecting the resilient modulus of base materials, correlation studies, and methods of determining the resilient modulus are described.
- *Section Three* describes the data collection and sample preparation of the base materials. This section also describes the experimental method of determining base properties.
- *Section Four* describes the data analysis in determining the multiple regression model, locally calibrated constitutive coefficients for NCHRP (2004) and Hicks and Monismith (1971) models using the linear and non-linear regression analysis.
- *Section Five* provides a summary, conclusions, and recommendations for future research work.

2. LITERATURE REVIEW

2.1 Introduction

This section summarizes a literature review of base materials for MEPDG. The standard properties of granular materials, resilient modulus, and factors affecting the resilient modulus are discussed. Furthermore, experimental methods of resilient modulus and correlation studies are presented in this section.

2.2 Background

Numerous research efforts have been devoted to characterizing the behavior of granular materials (Lekarp et al., 2000), which is one of the main concerns of pavement engineers. For a better understanding of this behavior, laboratory tests were performed at in-situ stress conditions and traffic loads. The simulation test protocol determines three nonlinear resilient modulus parameters (K_1, K_2 and K_3) of the NCHRP (2004) model. The resilient modulus test results are required in the Level 1 input of the MEPDG guide.

The design of proper and cost effective pavement structure requires an input of different variables and interactions that could affect the pavement performance. The guide for mechanistic-empirical design of new and rehabilitated pavement structures initiated by NCHRP (2004) requires the input of parameters for traffic, climate, and material affecting the pavement performance. One of the primary inputs required in the AASHTO pavement design software, AASHTOWare®, is the laboratory determined resilient modulus value of the base layer material that is presented in this section.

2.3 Properties Of Granular Materials To Cyclic Loading

Granular materials experience some non-recoverable deformations at the end of each cyclic loading. The degree of recoverable deformation increases more than non-recoverable deformation during the first few load applications (Figure 2.1). If the load is small compared to the strength of the material and repeated for many times, the deformation under each load application is nearly recoverable and proportional to the load that is considered using the elastic theory (Huang 1993). This behavior of granular materials is characterized as the resilient modulus. However, the excess energy creates non-recoverable strain after the load is released. The granular materials properties to repeat loading is shown in Figure 2.1.

The literature reviewed in this area shows that structural response and performance of conventional flexible pavements can be influenced by resilient modulus and permanent deformation accumulated in the granular materials. These parameters are typically determined by the repeated load triaxial testing method (Kancherla 2004).

The dynamic response of granular materials is usually characterized by the resilient modulus. The resilient modulus (M_r) given by Equation (2.1) is defined as the ratio of the repetitive deviator stress to the recoverable strain caused by the deviator and confining stress obtained from the repeated loading tri-axial test

$$M_r = \frac{(\sigma_1 - \sigma_3)}{\varepsilon_1} \quad (2.1)$$

where,

M_r = resilient modulus,

σ_1 = principal axial stress,

σ_3 = confining stress, and
ε_1 = axial resilient strain.

Further review indicated that granular pavement layers show a nonlinear and time dependent elastoplastic response under wheel loading (Lekarp et al., 2000).

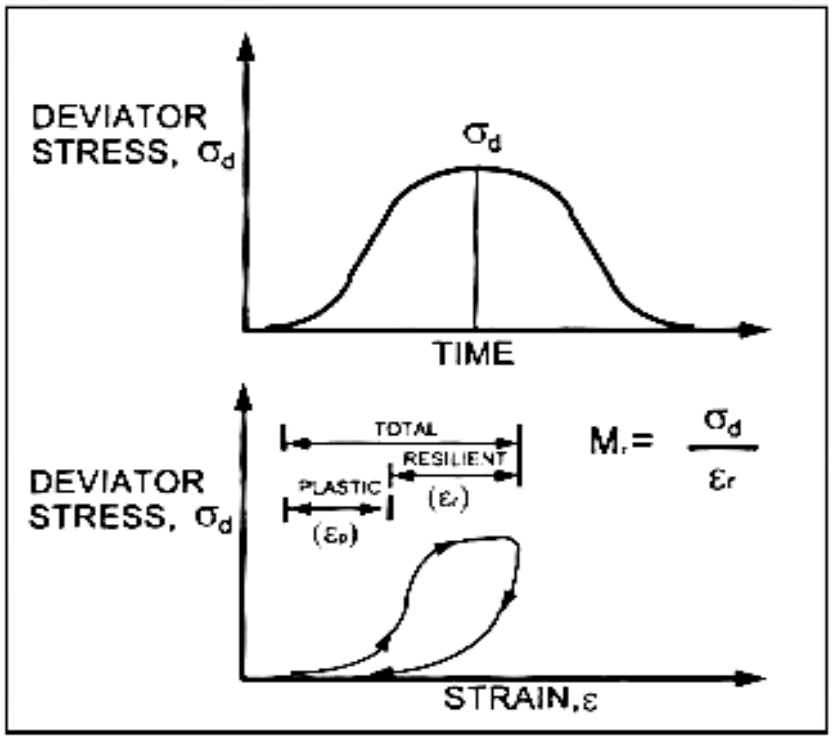

Figure 2.1 Strains in granular materials for the first initial load cycle (After Puppala 2008)

2.3.1 Parameters Affecting Resilient Modulus of Base Materials

The literature search for primary parameters affecting granular material properties during repetitive loading and unloading is discussed in this subsection. Parameters affecting the resilient behavior of base materials are a combination of index properties and engineering properties. The focus of the literature review for this category was the effects of stress, density, percent fines and grain size, aggregate gradation, moisture content, and aggregate type and shape on resilient modulus of base materials.

2.3.1.1 Confining, Axial, and Bulk Stresses

The resilient modulus of granular materials increases with an increase in confining and principal stresses. Numerous studies reviewed that the resilient modulus value has a very high degree of dependence on confining pressure and the sum of principal stresses for the resilient modulus (Mitry 1965; Hicks 1970; Uzan 1985; Sweere 1990). Monismith et al. (1967) reported that a change of confining stress from 2.9 to 29 psi (20 to 200 kPa), increased the resilient modulus by 500 percent, and in Smith and Nair (1973), there was an observed 50 percent increase in resilient modulus when the sum of principal stresses increases from 10 to 20 psi (70 to 140 kPa).

Both constant confining pressure (CCP) and variable confining pressure (VCP) were used in the tri-axial laboratory test method to investigate the effect of confining pressure. In Allen and Thompson (1974) it was reported that a higher resilient modulus was determined from the CCP test. However, in Brown and in Hyde (1975) it was concluded that both tests yield the same resilient modulus, providing the confining pressure in the CCP test is equal to the mean value of the pressure used in the VCP test.

Even though mean deviator and confining stresses are normally estimated for a pavement wheel load and pavement layer thickness, a representative stress level is also computed to determine the actual response of the pavement layer. Some researchers preferred to use the representative stresses instead of the AASHTO T 307 stress distribution protocol (Richard Ji et al., 2014). The representative stress values are computed for known wheel load and each pavement thickness above the level of interest.

2.3.1.2 Density

The impact of density on the resilient response of granular materials significantly changes with the degree of compaction and void content. Barksdale and Itani (1989) found that higher density of granular materials increases the stiffness, strength, and resilient modulus under a mean normal stress. However, at a high confining and deviatric stress level, the effect of density was found to be less pronounced. Vuong (1992) noted that the resilient modulus is not very sensitive to density as the density increases above the maximum dry density.

2.3.1.3 Percent Fines and Grain Size

From the literature review, the impact of percent fines was not quite clear on the stiffness of the materials. Nevertheless, some researchers, such as Barksdale and Itani (1989), reported a 60 percent decrease in resilient modulus for 0 to 10 percent increase in percent fines in the specimen. In Jorenby and Hick (1986), it was observed that an initial increase and a subsequent reduction in stiffness as clay-like fines were added to crushed aggregates. Ji et al. (2014) reported that an increase in percent fines in the granular test specimen significantly affects the constitutive coefficients of MEPDG resilient modulus models. The constitutive coefficient K_1 at 5 percent fines was found to be higher than that at 10 percent fines. However, the effects of 5 percent and 10 percent fines on the constitutive coefficients K_2 and K_3 were found to be very similar. In Mishra (2010), it was reported that percent fines equal to or more than 10 percent has a drastic effect on the performance of uncrushed materials.

Thom (1988) and Kolisoja (1997) investigated the effects of maximum particle size and grain size distribution of a similar aggregate shape on the resilient modulus. Both projects found that resilient modulus increased with increasing maximum particle size. According to the research outlined in *Gradation and Moisture Effects on Resilient Moduli of Aggregate Bases,* open graded aggregates (coarser gradation) have a higher M_r value and induce less damage to the pavement under a saturated condition (Tian et al. 2014).

2.3.1.4 Aggregate Gradation

Kolisoja (1997) reported that the particle size distribution or grading of granular materials seems to have some influences on material stiffness, although it is generally considered as a minor factor. Brown and Selig (1991), and Raad (1992) observed that uniformly graded aggregates were found to be slightly stiffer than well-graded aggregates. Thom and Brown (1988) studied the behavior of crushed limestone at different grading and concluded that the uniformly graded aggregates were only slightly stiffer than well-graded aggregates. Palaistow (1994) reported that grading has indirect effect on the resilient behavior of unbound aggregates by limiting the impact of moisture and density of the system.

Heydinger (1996) compared the effect of grading on resilient moduli of limestone, gravel, and slag. Limestone was found to have a higher resilient modulus at open graded than dense graded specification. However, well-graded (dense gradation) slag was found to have a higher resilient modulus than the open graded and could not trace the effect of gradation on gravel moduli.

2.3.1.5 Moisture Content

Degree of saturation of most untreated granular materials has been found to affect the response characteristics of the base materials in both laboratory and in-situ conditions (Lekarp et al. 2000). The resilient modulus of dry and most partially saturated granular materials was found to be similar. However, when a complete saturation is approached, the resilient modulus behavior may be affected significantly. A remarkable reduction in resilient modulus can be experienced as the degree of saturation increases (Smith and Nair 1973). Haynes and Yoder (1963) concluded that the resilient modulus of gravel decreased 50 percent when the degree of saturation increased from 70 to 97 percent.

Lekarp et al. (2000) mentioned that the pore pressure induced during load application was the main factor influencing the material behavior than the degree of saturation. However, Seed et al. (1967), Mitry (1965), and Hicks (1970) reported that the decrease in modulus due to saturation was obtained only if the analysis was based on total stresses. Pappin (1979) added that the resilient modulus remained approximately unchanged if the analysis was performed based on effective stresses.

Thom and Brown (1987) argued that the increase in the deformation of particles and the decrease in the resilient modulus were explained by the presence of lubricating effect on the particle. Tests were performed at a drained condition by increasing moisture content to 85 percent degree of saturation and loading frequency from 0.1 to 3 Hz. No pore water pressure was built up during the test when a considerable decrease in the resilient modulus was observed.

Raad (1992) reported that the decrease in resilient modulus due to moisture content is more significant on well-graded materials with high percent fines. According to recent research conducted by Ji et al. (2014), in Indiana, which discussed the effect of moisture content on resilient modulus, it was concluded that the effect of pore pressure suction is not significant to granular materials, unless a considerable amount of fines (5 - 10 percent) with high plastic limit exist in the sample. Furthermore, research done in Virginia, by Hossain and Lane (2015), concluded that moisture sensitivity was found on materials passing through sieves No. 40 and No. 200.

2.3.1.6 Aggregate Type and Shape

Many research studies concluded that crushed aggregates with angular to sub-angular particle shapes have higher resilient modulus than uncrushed gravel with sub-rounded or rounded particle shapes (e.g., Hicks and Monismith 1971; Allen 1973; Allen and Thompson 1974; Thom and Brown 1988; Barksdale and Itani 1989). Research conducted by Barsdale and Itani (1989), on rough angular crushed aggregates, showed a higher resilient modulus over rounded aggregates by 50 percent at a low mean normal stress and about 25 percent at a high mean normal stress. Even though increases in particle shape and roughness can yield higher resilient modulus, test results show that Poisson's ratio decreases for the same condition. The particle shapes were found to have a significant influence on resilient modulus (Kolisoja 1997).

According to a recent study conducted by Hossian and Lane (2015) in Virginia, due to its less affinity to moisture content, dolomitic limestone was found to have a higher resilient modulus than granite. Even though diabase is usually one of the hard rocks according to lithology, the resilient modulus was less than limestone. This may be due to the present of plastic fines on the diabase samples.

2.4 Correlation of Resilient Modulus

The most important mechanical property of granular materials that shows the dynamic distribution of stresses and strains within a pavement system is resilient modulus. Yet, even though the AASHTO Guide (1993) determined resilient modulus was not the preferred method, both AASHTO T 307 and NCHRP 1-37A recognize the need of compatibility of resilient modulus with past index properties of unbound materials to minimize the energy and resources required. Since the index properties were routinely used for the determination of pavement layer strength, a correlation of the resilient modulus and the index properties is highly recommended.

2.4.1 California Bearing Ratio Test (CBR) and R-Value test

California bearing ratio (CBR) and R-value are index properties of unbound materials to be presented in this section when discussing correlation with the resilient modulus. CBR is an indirect soil strength resistance measurement derived from penetrating unbound materials using a standardized piston moving at a standardized rate for a prescribed penetration distance. CBR has been correlated empirically with resilient modulus as summarized in Table 2.1. The AASHTO 1993 Design Guide correlation of resilient modulus with R-value and CBR of granular base and subbase layers is shown in Table 2.1.

Table 2.1 Correlation of resilient modulus with CBR and R-value (AASHTO 1993)

θ (psi)	**M_r (psi)~R**	**M_r (psi)~ CBR**
100	1000 + 780 × R	100740 × CBR
30	1000 + 350 × R	440 × CBR
20	1000 + 350 × R	340 × CBR
10	1000 + 250 × R	250 × CBR

Source: AASHTO (1993). θ–Bulk stress, R–R-value, CBR–California bearing ratio, and M_r–Resilient modulus.

R-value is a resistance measurement to soil deformation and is expressed as a function of the ratio of the induced lateral pressure to the applied vertical pressure measured in a triaxial type-loading device given by Equation (2.2)

$$R = 100 - \frac{100}{\left(\frac{2.5}{D_2}\right)\left(\frac{P_v}{P_h} - 1\right) + 1} \tag{2.2}$$

where,

R = resistance value,
P_v = applied vertical pressure (160 psi),
P_h = transmitted horizontal pressure (psi), and
D_2 = displacement of stabilometer fluid necessary to increase the horizontal pressure from 5 to 100 psi, measured in revolution of a calibrated pump handle.

Three hierarchical input levels of unbound material stiffness of flexible pavement types are available for the NCHRP 1-37A model. Level 1 requires direct laboratory measured resilient modulus values. Level 2 uses correlated resilient modulus in terms of other index properties. Level 3 uses default resilient modulus values based on soil type. The correlated resilient modulus for Level 2 inputs can be determined using the relationships summarized in Table 2.2.

Table 2.2 Correlation models for resilient modulus (NCHRP 1-37A, 2004)

Strength/ Index Property	Model	Comments
CBR	$M_r = 2555(CBR)^{0.61}$	CBR = California Bearing Ratio in percent
R- value	$M_r = 1155 + 555R$	R = R-value
AASHTO layer coefficient	$M_r = 30000\left(\frac{a_i}{0.14}\right)$	a_i = AASHTO layer coefficient

Note: CBR measured at optimum moisture and density Verses soaked conditions of M_r at corresponding moisture and density conditions.

The default resilient modulus for Level 3 inputs recommended by the NCHRP 1-37A, as per AASHTO soil classification, is summarized in Table 2.3.

Table 2.3 Default resilient modulus as per soil classification for Level 3 inputs (NCHRP 1-37A, 2004)

AASHTO Material Classification	M_r Range (psi)	Typical M_r (psi)
A-1-a	38,500 - 42,000	40,000
A-1-b	38,500 - 40,000	38,000
A-2-4	28,000 - 37,500	32,000
A-2-5	24,000 - 33,000	28,000
A-2-6	21,500 - 31,000	26,000
A-2-7	21,500 - 28,000	24,000
A-3	24,500 - 35,000	29,000

2.5 Laboratory Test Methodology

The two common test procedures used to determine the resilient modulus property of base materials are found in NCHRP 1-28A (2004) and AASHTO T 307 (2007). The AASHTO T 307 (2007) procedure modified by WYDOT in 2015 for this study was also described in the master thesis by Henrichs (2015).

2.5.1 Harmonized Test Protocol (NCHRP 1-28A)

The harmonized test method was developed from research project NCHRP 1-28A, to determine resilient modulus for a flexible pavement design. One of the main objectives of the research was to develop a test method by harmonizing the procedure proposed by NCHRP Project 1-28A considering AASHTO TP31 (1996) and the FHWA LTPP laboratory start up and quality control procedure (Andrei 2004). Since this research focuses on resilient modulus of base material, only the methods pertaining to base materials are presented.

The test procedure for laboratory preparation and testing method described by NCHRP 1-28A was adopted from AASHTO T 294 (1992), TP 46 (1994) and T 292 (1991). The stress level for different

layers is based on their depths with respect to the top pavement surface layer. The size of the specimen depends on the maximum nominal particle size of the sample material to be tested.

The resilient modulus procedure proposed by NCHRP 1-28A is based on the grain size distribution and plasticity index property of sample materials. The material can be classified in four types (Type 1, Type 2, Type 3 and Type 4). Type 1 and Type 2 represent the base and subbase materials, and Type 3 and Type 4 represent the subgrade materials. Type 1 includes all unbound granular base and subbase materials with maximum particle sizes greater than 0.375 inch (9.5 mm). Type 2 has a maximum particle size less than 0.375 inch (9.5 mm) and less than 10 percent passing the No. 200 sieve.

The duration of test method loading waveform is 0.1 second of the load pulse followed by 0.9 seconds of rest period. The contact load is 20 percent of the confining load, and the stress-strain combination goes to 30 sequences with a constant ratio of the confining to the maximum axial load.

2.5.2 AASHTO T 307 (2007)

The AASHTO T 307 (2007) describes the sample preparation and testing of untreated base/subbase materials for the determination of M_r. The wheel loads are simulated to the stress state and physical condition of the layer below the flexible pavement to determine the resilient modulus. The resilient modulus is explained as the measure of the elastic modulus recognizing certain non-linear characteristics. This method is the basis for resilient modulus testing currently adopted by state DOTs.

According to AASHTO T 307, materials are classified as Type 1 and Type 2. Type 1 materials include all untreated granular base/subbase materials less than 70 percent passing No. 10 sieve, less than 20 percent passing No. 200 sieve and with a plastic index of 10 or less. All materials not meeting the criteria of Type 1 are classified as Type 2. The diameter of Type 2 undisturbed cohesive specimens is 2.8 inch or 3.39 inch (71 mm or 86 mm). The selected mold size of Type 1 specimen or compacted specimens of Type 2 is a minimum diameter equal to five times the maximum particle size. If the maximum particle size exceeds 25 percent of the largest mold diameter available, these particles shall be removed, and the length for all specimens shall be at least two times of the diameter.

In order to simulate the moving wheel load on the test specimen, a repeated axial cyclic stress of fixed magnitude, confining stress followed by the load duration, and at different sequences are applied to determine the representative resilient modulus. AASHTO T 307 requires a tri-axial pressure chamber and two external spring-loaded linear variable transducers (LVDTs) to measure the recoverable axial strain. The corresponding cyclic stress pulse is a haversine shaped load in the form of $(1-\cos\theta)/2$. The time interval for the specimen subjected to a cyclic stress is 1.0 to 3.1 second, and axial cyclic stress of fixed magnitude load duration is 0.1 second.

According to AASHTO T 307, all unbound granular base and subbase materials are compacted to approximate in-situ wet density and moisture content. However, if the in-situ material property is not readily available, the maximum dry density and the corresponding optimum moisture content in accordance with AASHTO T 99 (2010) or T 180 (2015) specified by the individual testing or transportation agency will be used. The moisture content of the laboratory-compacted specimen shall not vary from the target moisture content by more than ±1.0 percent for Type 1 materials or ±0.5 percent for Type 2 materials. In addition, the wet density of the laboratory-compacted specimen shall not vary by more than ±3 percent of the target-wet density. Once the proper amount of sample is prepared and mixed with the target moisture content, the soil sample must be sealed in a plastic bag or container with a tight lid from 16 to 48 hours of hydration time. After hydration, the sample is ready for compaction.

Vibratory compaction method is suggested for both Type 1 and Type 2 materials. The electric rotary or demolition hammer with a rated input of 750 to 1250 watts and capable of 1800 to 3000 blows per minute shall be used. Detail information can be found in the AASHTO T 307 ANNEX B3.

2.5.2.1 Base/Subbase Material testing

After compaction of the specimen is completed, the filter, porous bronze disc and specimen cap are placed on the top surface. The rubber membrane is rolled off the rim of the mold and over the sample cap. The membrane shall be sealed tightly against the cap with the O-ring seal. Then the specimen is placed in the triaxial testing machine and the pressure chamber supply line is connected. The axial loading device or triaxial chamber base support is necessary to adjust with the load-generation device piston and the tri-axial chamber piston. This procedure will help the tri-axial chamber piston to bear firmly on the load cell.

After applying a confining pressure of 15 psi (103.4 kPa), the vacuum supply is removed from the saturation inlet. The top and bottom drainage ports are opened to atmospheric pressure, and constant stress of 10 percent ± 0.1 psi (0.7 kPa) of the maximum applied stress during each sequence number shall be maintained. The loads applied to the top of the triaxial cell piston rod shall be adjusted to the stresses shown in Table 2.4.

Table 2.4 Testing sequences for Base/Subbase Materials (AASHTO T 307, 2007)

Sequence No.	Confining Pressure		Maximum Axial Stress		No. of Load Applications
	kPa	psi	kPa	psi	
0	103.4	15	103.4	15	500-1000
1	20.7	3	20.7	3	100
2	20.7	3	41.4	6	100
3	20.7	3	62.1	9	100
4	34.5	5	34.5	5	100
5	34.5	5	68.9	10	100
6	34.5	5	103.4	15	100
7	68.9	10	68.9	10	100
8	68.9	10	137.9	20	100
9	68.9	10	206.8	30	100
10	103.4	15	68.9	10	100
11	103.4	15	103.4	15	100
12	103.4	15	206.8	30	100
13	137.9	20	103.4	15	100
14	137.9	20	137.9	20	100
15	137.9	20	275.8	40	100

If the total vertical permanent strain exceeds the 5 percent deformation during the preconditioning, the test shall be terminated, and the specimen shall be prepared again. At the end of the 15th sequence, the load and the confining pressure are reduced to zero and followed by a quick shear test. This procedure is performed at 5 psi (34.47 kPa) confining pressure until the sample is failed to determine the maximum failure load.

After completion of the resilient modulus testing, report forms are prepared to summarize the test results. The forms shall show the recorded loads, stresses, deformation, resilient modulus values for each sequence of last five pulses and record the physical data of the specimen, such as the height, diameter, moisture, and unit weight.

2.6 WYDOT Testing Protocol

The WYDOT modified AASHTO T 307, explicitly described in the master thesis by Henrichs (2015), for resilient modulus of base materials with a mold size of four inches is used in this study**.** The testing apparatus and compaction method stated within the WYDOT Modified AASHTO T 307 shall be used in testing "W" and "L" grading of the base aggregate materials described in Section 3.2. The compaction method in the AASHTO T 307 is modified, and additional reporting form for the resilient modulus test is also prepared.

2.7 M_r Constitutive Models

The nonlinear resilient behavior of base materials affected by the parameters discussed in Section 2.3.1 creates challenges for researchers to correlate the theoretical principles of soil mechanics with the material response. Therefore, the complex behavior of the materials has been described using constitutive models. In addition, computational models have been developed to account for the dynamic properties of pavement materials.

The concept of resilient modulus has been used to explain the nonlinear stress-strain characteristics of the pavement layer materials. Numerous constitutive models have been proposed by many researchers for modeling the dynamic response of the pavement materials. The most commonly used constitutive models, which are summarized in the following equations, relate the resilient modulus with the bulk stress, deviator stress, and both deviator and octahedral stresses.

A simple model developed by Hicks and Monismith (1971), Equation (2.3), considers the effect of bulk stress when addressing the nonlinear behavior of the base material.

$$M_r = K_1 \theta^{K_2} + \varepsilon \tag{2.3}$$

where,

M_r = resilient modulus (psi)
θ = bulk stress (psi),
K_1, K_2 = material regression coefficients, and
ε = population error.

Equation (2.4), developed by Uzan (1985), includes the bulk stress and deviator stress with respect to the atmospheric pressure in the determination of resilient modulus.

$$M_r = K_1 P_a \left(\frac{\theta}{P_a}\right)^{K_2} \left(\frac{\sigma_d}{P_a}\right)^{K_3} + \varepsilon \tag{2.4}$$

where,

M_r = resilient modulus (psi),
θ = bulk stress (psi),
σ_d = deviator stress (psi),
P_a = atmospheric pressure of 14.7 psi (101.3 kPa) used to make the stresses non- dimensional parameter, and
$K_1, K_2,$ and K_3 = multiple regression coefficients.

The next model, Equation (2.5), is known as the universal model, and was developed by Uzan (1992), which includes the octahedral shear stress instead of the deviator stress.

$$M_r = K_1 \left(\frac{\theta}{P_a}\right)^{K_2} \left(\frac{\tau_{oct}}{P_a}\right)^{K_3} + \varepsilon \quad (2.5)$$

where,

$\theta = \partial_1 + \partial_2 + \partial_3 = \partial_1 + 2\,\partial_3$ = bulk stress (psi),
$\partial_d = \partial_1 - \partial_3$= deviator stress (psi),
$\tau_{oct} = \frac{1}{3}\sqrt{(\partial_1 - \partial_2)^2 + (\partial_1 - \partial_3)^2 + (\partial_2 - \partial_3)^2}$ = octahedral shear stress (psi),
P_a = atmospheric condition or unit reference pressure equal to 14.7 psi (101.3kPa), and
K_1, K_2 and K_3 = multiple regression coefficients.

Cary and Zapata (2011) also developed a model that takes into account the matrix suction effect of pore water pressure generated under the moving wheel loads. One of their objectives was to include matric suction as a predictive parameter in the universal model given by

$$\mathbf{M_r = K'_1 p_a \left(\frac{\theta_{net} - 3.\Delta\mu_{w-sat}}{P_a}\right)^{K'_2} \left(\frac{\tau_{oct}}{P_a} + 1\right)^{K'_3} \left(\frac{(\psi_{mo} - \Delta\psi_m)}{P_a} + 1\right)^{K'_4} + \varepsilon} \quad (2.6)$$

where,

M_r = resilient modulus (psi),
$\theta_{net} = \theta - 3\mu_a$, net bulk stress and $\mu_a$is pore air pressure (psi),
$\Delta\mu_{w-sat}$= build-up of pore water pressure under saturated conditions (psi),
$K'_1 \geq 0, K'_2 \geq 0, K'_3 \leq 0,$ and $K'_4 \geq 0$ are regression coefficients,
P_a= atmospheric pressure (psi),
τ_{oct}= octahedral shear stress (psi),
ψ_{mo}= initial matrix soil suction (psi), and
$\Delta\psi_m$= relative change of matrix soil suction with respect to ψ_{mo} due to build-up of pore water pressure under unsaturated conditions.

The latest model developed by NCHRP 1-37A (2004), and adopted in the MEPDG, is shown in Equation (2.7). This model is similar to the universal model, Equation (2.5), except 1 is added to the octahedral shear stress in order avoid zero modulus when the octahedral stress is zero.

$$M_r = K_1 P_a \left(\frac{\theta}{P_a}\right)^{K_2} \left(\frac{\tau_{OCT}}{P_a} + 1\right)^{K_3} + \varepsilon \quad (2.7)$$

In this study, the models shown in Equation (2.3) and Equation (2.7) were used in determining the constitutive regression coefficients for the level-2 M_r value input.

3. RESILIENT MODULUS EXPERIMENT

3.1 Introduction

This section describes the source of base materials, summary of standard properties, laboratory setup, test matrix, aggregate shape, and soil classification for this project. WYDOT modified AASHTO T 307 was selected as the laboratory testing procedure for resilient modulus.

3.2 Source of Base Materials and Standard Properties

Base materials were collected throughout Wyoming to characterize the local crushed base properties. The sample materials were collected from WYDOT road projects completed in 2015 and 2016. These collected samples were selected by WYDOT for laboratory testing. Fourteen aggregate sources were initially selected; however, one of the sources (Reiter Pit) could not satisfy the R-value requirement for base material and another two sources (Hay Hill Pit and Patty Pit) did not have enough aggregate quantity for laboratory testing. The WYDOT gradation system of base materials is shown in Table 3.1 (WYDOT 2017).

Table 3.1 WYDOT gradation system (WYDOT Specification Table 803.4.4.-1, 2017)

Sieve		**Grading (Percent Passing)**					**R-value**
mm	**inches**	**J**	**GR**	**L**	**K**	**W**	
50	2	100	-	-	-	-	≥75
37.5	1.5	90 - 100	-	100	100	100	
25	1	-	100	90 -100	90 - 100	90 - 100	
19	0.75	-	90 -100	-	-	-	
12.5	0.5	-	65 - 85	60 - 85	-	60 - 85	
9.5	0.375	-	-	-	-	-	
4.75	#4	35 - 75	50 - 78	35 - 55	40 - 65	45 - 65	
2.36	#8	-	37 - 67	25 - 50	30 - 55	33 - 53	
0.6	#30	-	13 - 35	10 - 30	-	-	
0.075	#200	0 - 15	4 - 15	3 - 15	3 - 15	3 - 12	

Figure 3.1 displays the locations of 14 aggregate sources used in this project.

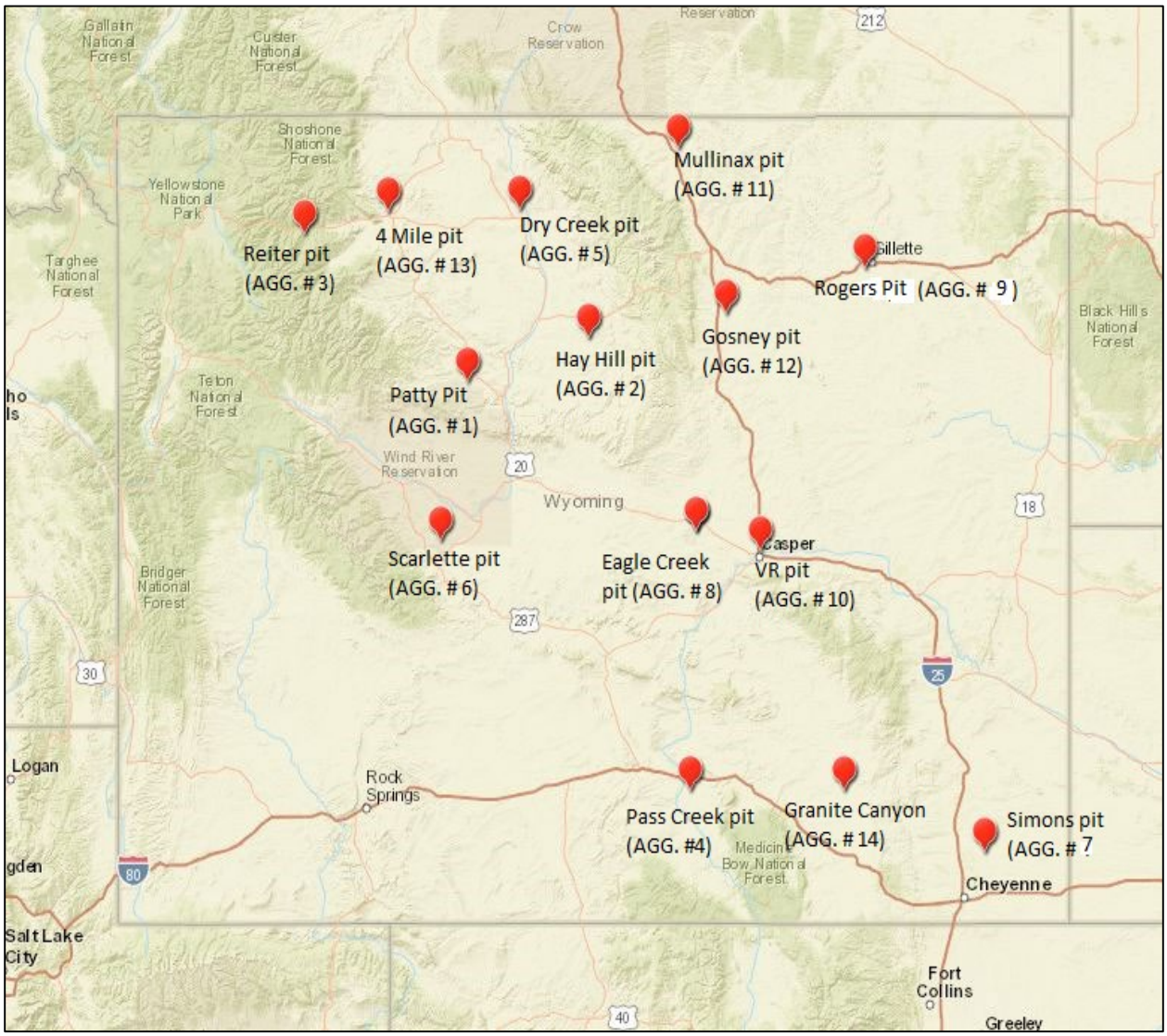

Figure 3.1 Locations of 14 aggregate sources

The standard properties of base materials include the gradation, density-moisture relationship determined in accordance with AASHTO T 99 (2010), crushed base grading according to WYDOT specification, and R-value according to ASTM of WYDOT standard testing plan. These properties were determined by the WYDOT Materials & Testing Program. Table 3.2 and Table 3.3 summarize the source locations, pit sources, standard properties, and R-values of 14 aggregate sources. Based on the WYDOT gradation shown in Table 3.1, 11 samples were classified as grading "W" while the remaining three were classified as grading "L". The combination of the pit run and the crushed run aggregates were done in the field by the contractors or by the WYDOT personnel at WYDOT materials laboratory. If the percentage of pit run to the crushed run was not known, the gradation was named as field combined gradation in this study.

Table 3.2 Locations, pit sources, and standard properties of base materials

AGG. #	Location	Pit Source	Gradation (Percent)		One Fracture Face (%)	WYDOT Grading (W/L)	Percent Passing #200	LL	PI
			CR	PR					
AGG-1 (Type-1)	Hot Spring	Patty Pit	60	40	NA	W	9.64	NV	NP
AGG-2 (Type-1)	Cheyenne/ Thermopolis	Hay Hill Pit	55	45	65	W	9.7	NV	NP
AGG-3 (Type-1)	Park County	Rieter Pit	Field Combined Gradation		76	W	5.2	NV	NP
AGG-4 (Type-1)	Carbon County	Pass Creek Pit	Field Combined Gradation		NA	W	5.9	NV	NP
AGG-5 (Type-1)	Big Horn County	Dry Creek Pit	100	0	84	W	11.9	NV	NP
AGG-6 (Type-1)	Fermont County	Scarlett Pit	55	45	NA	W	6.6	NV	NP
AGG-7 (Type-1)	Laramie County	Simon's Pit	Field Combined Gradation		90	W	6.4	NV	NP
AGG-8 (Type-2)	Casper-Natrona County	Eagle Creek Pit	Field Combined Gradation		100	L	5.8	22	3
AGG-9 (Type-1)	District-4 Bridge Rehab	Rogers Quarry	Field Combined Gradation		100	L	9.4	NV	NP
AGG-10 (Type-1)	Casper-Natrona County	VR Pit	Field Combined Gradation		83	W	9.4	NV	NP
AGG-11 (Type-1)	Sheridan County	Mullinax Pit	Field Combined Gradation		85	W	8.5	NV	NP
AGG-12 (Type-1)	Kaycee Buffalo	Gosney Pit	Field Combined Gradation		NA	W	11.1	NV	NP
AGG-13 (Type-1)	Cody-Park County	4 Mile Pit	Field Combined Gradation		84	W	7.3	NV	NP
AGG-14 (Type-1)	Laramie Albany County	Granite Canyon Quarry Pit	Field Combined Gradation		100	L	8.5	NV	NP

AGG. # −Aggregate, CR−Crushed Run, PR−Pit Run, W−Aggregate Gradation, L−Aggregate Gradation, LL−Liquid Limit, PI−Plastic index, NV−Non-viscous, and NP−Non-plastic.

Table 3.3 Standard Proctor test results and R-value results of base materials

AGG. #	Location	Pit Source	Opt. M.C (%)	Max. Dry Density (pcf)	M.C for R value test (%)	R-value	R-value at 300 psi	AASHTO Soil Classification
AGG -1 (Type-1)	Hot Spring	Patty Pit	5.9	136.5	6.7	80	78	A-1-b
					7.9	79		
					9.2	65		
AGG -2 (Type-1)	Cheyenne/ Thermopolis	Hay Hill Pit	6.6	139.6	6.6	84	77	A-1-b
					8.3	79		
					9.9	73		
AGG- 3 (Type-1)	Park County	Rieter Pit	6.8	135.7	6.6	66	66	A-1-a
					8.3	67		
					9.5	66		
					10.8	66		
AGG – 4 (Type-1)	Carbon County	Pass Creek Pit	6.1	141.1	4.9	85	76	A-1-a
					6.6	76		
					8.3	81		
AGG – 5 (Type-1)	Big Horn County	Dry Creek Pit	6.6	137.9	4.9	82	76	A-1-a
					6.6	76		
					8.3	74		
AGG - 6 (Type-1)	Fermont County	Scarlett Pit	6	138.1	6.7	83	79	A-1-a
					9.2	79		
					11.7	72		
AGG -7 (Type-1)	Laramie County	Simon's Pit	6.4	138.7	6.7	75	75	A-1-a
					7.9	75		
					9.2	71		
AGG-8 (Type-2)	Casper-Natrona County	Eagle Creek Pit	6	142.9	5.8	92	88	A-1-a
					7.5	89		
					8.3	88		
					9.2	87		
AGG-9 (Type-1)	District-4 Bridge Rehab	Rogers Quarry	6.0	140.7	5.8	79	79	A-1-a
					8.3	79		
					9.9	77		
AGG-10 (Type-1)	Casper-Natrona County	VR Pit	6.1	141.7	5.0	87	85	A-1-a
					6.7	85		
					7.5	82		
AGG-11 (Type-1)	Sheridan County	Mullinax Pit	6.8	139.6	5.8	92	86	A-1-a
					7.5	89		
					9.2	76		
AGG-12 (Type-1)	Kaycee Buffalo	Gosney Pit	6.2	1393.3	5.8	83	76	A-1-a
					6.7	78		
					7.5	75		
					8.3	75		
AGG-13 (Type-1)	Cody-Park County	4 Mile Pit	6.2	140.7	5.8	83	80	A-1-a
					7.1	83		
					8.3	73		
AGG-14 (Type-1)	Laramie-Albany County	Granite Canyon Quarry Pit	6.3	143.4	3.3	85	76	A-1-a
					6.7	75		
					8.3	77		

AGG. # −Aggregate, Opt. M.C−Optimum Moisture content, and M.C−Moisture content.

3.3 Laboratory Testing

The crushed base samples were classified in accordance with the AASHTO T 307 base/subbase (Type 1 or Type 2) classification systems. The resilient modulus (M_r) test was conducted following the WYODT modified AASHTO T 307 procedure specifically developed for WYDOT by Henrichs (2015).

All the selected base materials for laboratory testing were found to be Type 1, and WYDOT was responsible for determining the gradations and R-values of base samples. The R-value test was conducted using a stabilometer on all selected crushed base materials. The research team used WYDOT's cyclic triaxial testing equipment to determine the M_r value of each source aggregate. Detailed descriptions of sample preparation, compaction, reporting, and aggregate shape with respect to the AASHTO soil classification system are presented in the following subsections.

3.3.1 Sample Preparation

The specimen was prepared by strictly following the modified AASHTO T 307 (2014) to consider the existing standards, specifications used by WYDOT, the testing equipment, and construction practices. Each specimen was prepared in a 4-inch diameter and 8-inch height mold shown in Figure 3.2. The maximum nominal aggregate size used was ¾ inch. Each sample was prepared at four different moisture contents (two below, optimum and one above optimum) in order to evaluate the effect of moistures on the M_r-value. After thoroughly blended the required sample aggregate with water to reach the target moisture content, the sample was placed in a sealed plastic container as shown in Figure 3.3. The container was kept in a room temperature for 16 to 24 hours to achieve a complete hydration of the samples. According to the gradation sheet, the aggregates are weighed and mixed with the required amount of water and placed in the plastic storage container as shown in Figure 3.3.

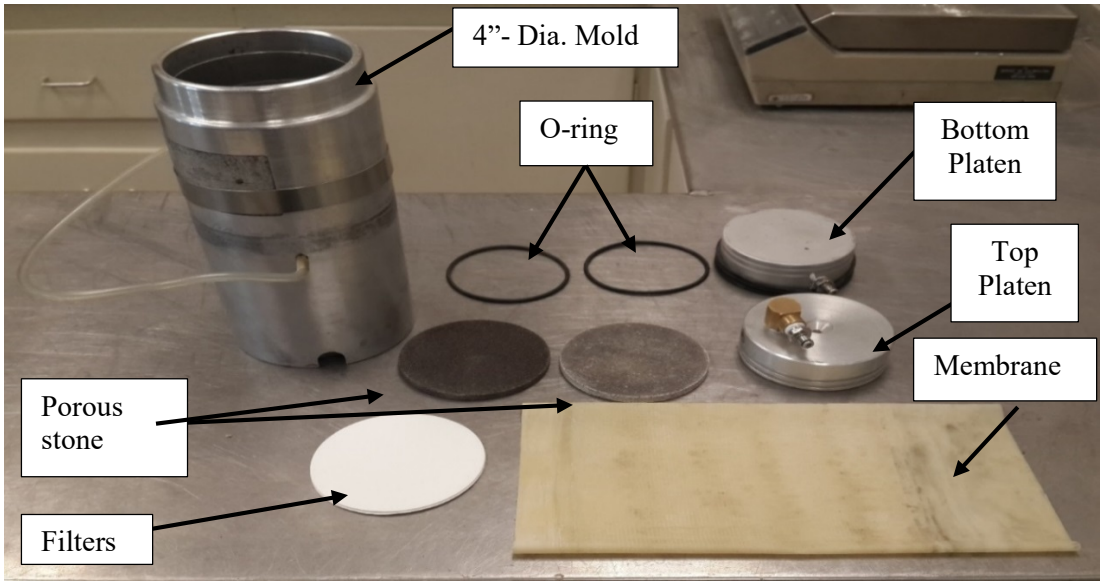

Figure 3.2 Four-inch diameter mold and other apparatus (Mebrahtom 2017)

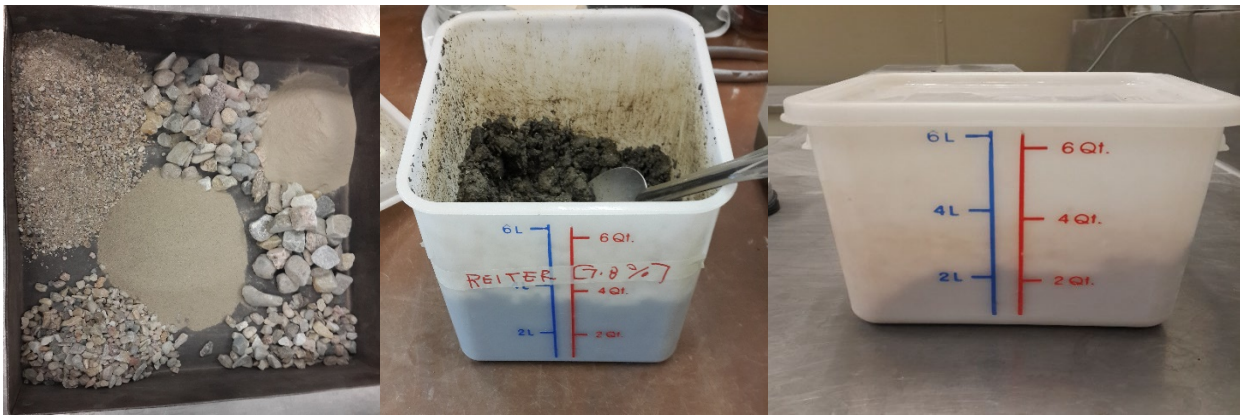

Figure 3.3 Sample weighed, mixed with water, and stored in a container for hydration (Mebrahtom 2017)

3.3.2 Compaction

After the sample was completely hydrated, the compaction was performed using the vibratory rotary compactor available at WYDOT, shown in Figure 3.4. The compaction procedure was done by first determining the thickness and weight of the bottom and top platens, two wet porous stones, two O-rings, two filter papers, and two plastic membranes. The membrane was fixed to the bottom platen using two O-rings. Next, the porous stone and filter paper were placed inside the mold over the membrane. The platen was tightly placed on the base of the vibratory compactor, and a vacuum line was connected to the mold to ensure a good contact between the membrane and the mold. To avoid pinching the membrane during placement of the split mold around the bottom platen, careful placement of the mold is required. The membrane is stretched tightly over the rim of the mold, and to draw the membrane in contact, a sufficient vacuum was applied. The use of a porous plastic forming jacket line between the split mold and the membrane improved the smoothness of the membrane with the split mold wall. To determine the volume (V) of the prepared specimen, the inside diameter of the membrane-lined mold and the height between the lower porous stone and the top of the mold were measured to the nearest 0.01 inch (0.25 mm). The compaction steps, starting from sample weighing to final compaction of the sample, are illustrated in Figure 3.5.

To achieve the desired density and achieve a uniform density over the specimen depth, the mass of the material was compacted in multiple lifts. Since all the material sources were classified as Type 1, the vibratory compaction was completed in six lifts as per AASHTO T 307 sample compaction procedure. The mass for each of the six layers (W_L), to be compacted in 4-inch (152-mm) diameter specimens and 8-inch (203.2 mm) height, was determined by Equation (3.1)

$$\mathbf{W_L} = {}^{\mathbf{W_t}}/_{\mathbf{N}} \tag{3.1}$$

where,

W_t = total mass of test specimen to produce the appropriate density (gram),
W_L = mass of each layer to be compacted (gram), and
N = number of layers to be compacted.

Next, the weighted mass of wet soil (W_L) was carefully placed into the mold center and vibrated until the distance from the surface of the compacted layer to the rim of the mold equaled the previously measured height, minus the thickness of the layer selected. After scarifying the already compacted layer to 0.12 inch (3 mm), the compaction process was repeated for the remaining layers. When the compaction was

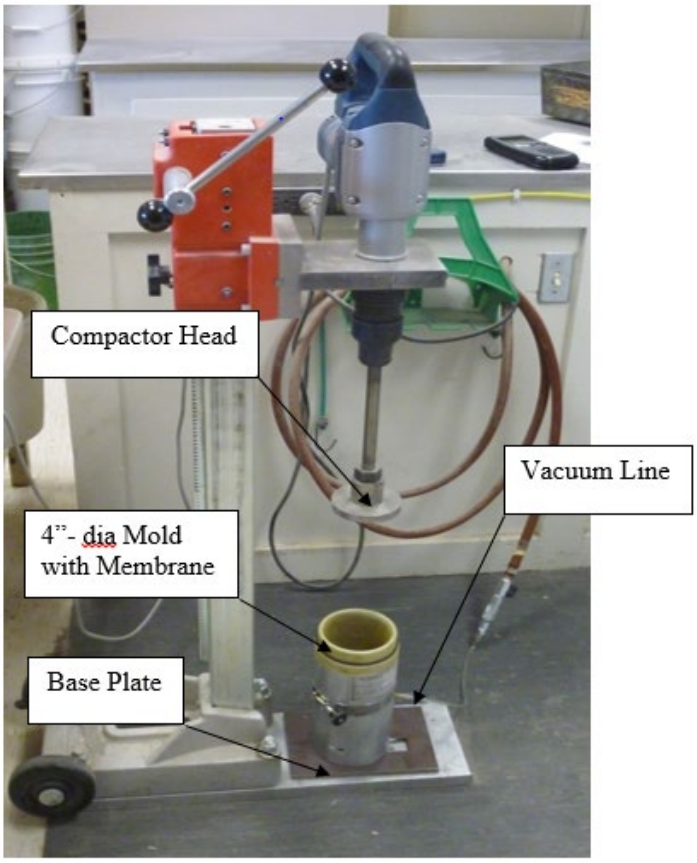

Figure 3.4 WYDOT vibratory compaction apparatus (Mebrahtom 2017)

Figure 3.5 Sample Compaction steps (Mebrahtom 2017)

completed, the split mold was removed, and the loose material from the top sample was cleared. After placing the filter paper, porous stone, top cap, and the second plastic membrane fixed with the O-rings, the total specimen mass was measured. The mass of the specimen, the excess soil, and pan were weighed and subtracted from the previous measured sample data. The loss of moisture content from the wetted soil during compaction can be avoided by covering the pan with a lid. The moisture content of this sample

was determined using AASHTO T 265 protocol. When the compaction process was completed, the sample was placed in the triaxial chamber for M_r testing.

3.3.3 M_r testing

The M_r testing was conducted at the laboratory of WYDOT Materials & Testing Program. The triaxial chamber and an Interlaken series 3300 Test frame, manufactured by Interlaken Technology Corporation (ITC), are shown in Figure 3.6. The triaxial chamber was equipped with two (top and bottom) loading cells and two spring-loaded linear variable differential transducers (LVDTs) that record the axial recoverable deformations of the specimen. A computer was also installed with a software program called ITC UniTest that controls the loading sequences and records all the measurements for the calculation of the M_r value. The M_r value is calculated by dividing the measured deviator stress to the average recoverable strain obtained from the two LVDTs.

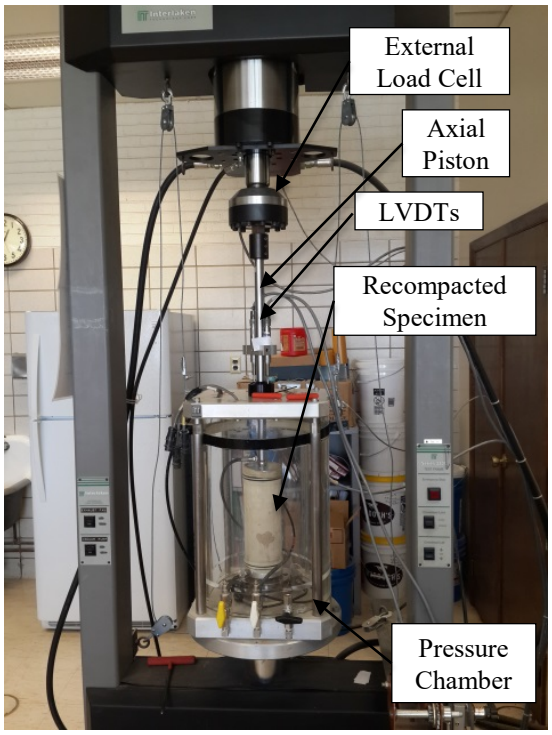

Figure 3.6 Triaxial chamber and test frame at WYDOT Materials and Testing Laboratory used for M_r Testing (Mebrahtom 2017)

The resilient modulus testing equipment was verified on a plastic trial sample and soil sample before the actual sample testing was completed. The triaxial chamber, loading sensors, and LVDT's were calibrated by Calibration Certification (Cal-Cert) before the study was conducted. After the calibration of the equipment was completed, the testing of a plastic specimen was performed two times. The resilient moduli produced by the testing equipment were realistic and repeatable.

3.3.4 Reporting

The physical measurement recording and hand calculation worksheet developed by Henrichs (2015) was modified and used for the M_r laboratory testing of base materials. Figure 3.7 is the sample worksheet used by WYDOT for testing lab crushed base resilient modulus.

WYOMING DEPARTMENT OF TRANSPORTATION MATERAIL TESTING LAB
CRUSED BASE RESILIENT MODULUS TESTING WORKSHEET

Date:	7/25/2016	Location:	SCARLETTE PIT
Engineer:	Dr. Kam Ng	Project/Site:	FERMONT
Tested by:	Dawit	Lab No:	202014

INITIAL DATA

Max. Dry Density:		138.1	lbs/ft^3
Opt. Moisture:		6	%
x	laboratory		in-situ
Min. Density:	95%	131.2	lbs/ft^2

SOIL BATCH DATA

Target Moisture:	6	Optimum
Target Density:	138.1	lbs/ft^3
Initial Moisture %:	0.0	%
% Moisture to Add:	6.0	%
	grams	lbs
Weight of Soil:	3764.8	8.30
Weight of Water:	225.9	0.50
Total Batch Weight:	8.22	lbs
Weight Per Lift: (6 Lifts)	1.37	lbs

RESILIENT MODULUS OUTPUT

Sequence	psi Chamber Confining Pressure	psi Nominal Max. Axial Stress	psi Resilient Modulus
1	3.0	3.0	11767
2	3.0	6.0	13429
3	3.0	9.0	15587
4	5.0	5.0	16780
5	5.0	10.0	19542
6	5.0	15.0	22114
7	10.0	10.0	27316
8	10.0	20.0	31813
9	10.0	30.0	33593
10	15.0	10.0	32752
11	15.0	15.0	34423
12	15.0	30.0	39358
13	20.0	15.0	40468
14	20.0	20.0	41693
15	20.0	40.0	46548
Was 5% deformation reached?			No

MEASURED DATA

Membrane Thickness 1 :	0.012	in
Membrane Thickness 2 :	0.012	in
Top Dia:	4.00	in
Center Dia:	3.96	in
Bottom Dia:	3.97	in
Total Height After comp.:	11.25	in
H of cap, stone, filter:	3.37	in
T. H at end of Mr test:	11.25	in
Δ H(< 5% Deformation):	0.00	OK
Total Weight:	12.321	lbs
W of cap, stone, filter:	4.153	lbs
W of sample aft. Comp.	8.168	lbs

MOISTURE CONTENT

	Initial	Final	
Wet W + Tare:		201.1	g
Tare:		29.9	g
Dry W + Tare:		191.1	g
Wet W:		171.2	g
Dry W:		161.2	g
% Moisture:	0.0	6.2	%

CALCULATED VALUES

Sample Diameter:	3.95	in
Sample Height:	7.88	in
Sample Weight:	8.17	lbs
Sample Volume:	0.056	ft^3
Moist Unit Weight:	146.0	lbs/ft^3
Dry Unit Weight:	137.4	lbs/ft^3

OVERALL RESULTS

Classification:	Type-1
Material Type (1 or 2)	A-1-a
R - Value: (CB)	79
M_R - Value:	28478.87 psi
Quick Shear	
Max. Shear Strength	5.14 psi
Did sample fail in shear?	No

Figure 3.7 Sample worksheet of a crushed base resilient modulus test result (Mebrahtom 2017)

3.4 Aggregate Shapes and Soil Classification

Most local crushed base materials collected in Wyoming have a combined gradation of the pit run, and the crushed run aggregates, except Dry Creek Pit that has 100 percent crushed run aggregates. The pit run aggregates were composed of round, smooth, and slate aggregates as shown in Figure 3.8a. The crushed run aggregates were rough and angular with 85 to 90 percent single face fractured as shown in Figure 3.8b.

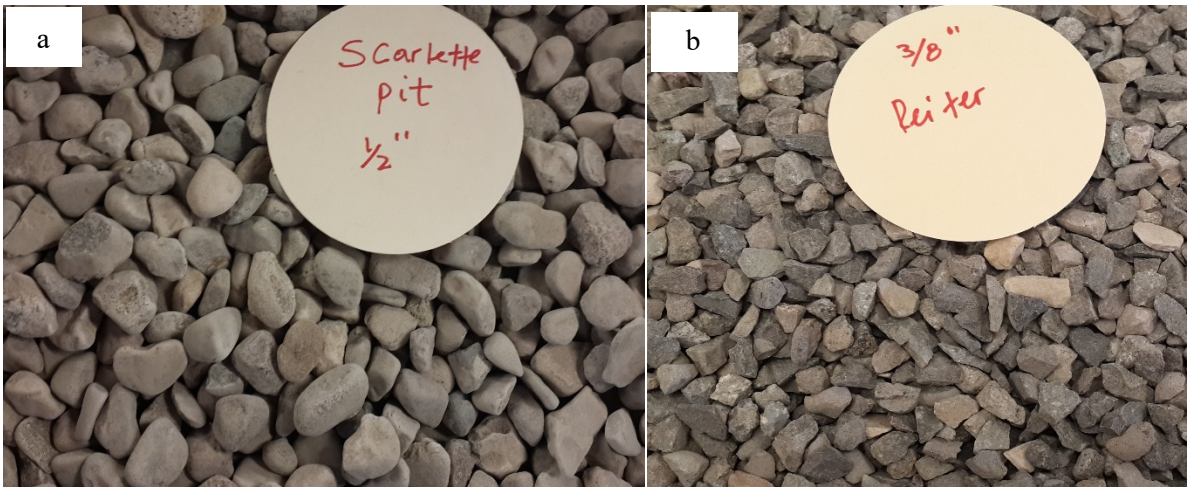

Figure 3.8 Local base materials composed of (a) pit run and (b) crushed run aggregate (Mebrahtom 2017)

The WYDOT specifications allow combination of the pit run with the crushed run aggregates to meet the base/subbase grading requirement. Even though WYDOT practices do not incorporate the No. 10 and No. 40 sieve sizes in the sieve analysis for base/subbase materials, the percent passing between No. 8 and No.16 sieves were from 40 to 50 percent, and for No. 30 sieve, the percent passing was below 30 percent for all the samples. Therefore, the AASHTO Soil Classification System was used to get the soil class. The Patty Pit and Hay Hill Pit aggregate sample sources were classified as A-1-b, while the rest were classified as A-1-a in accordance with the AASHTO Soil Classification System.

4. RESULTS AND STATISTICAL ANALYSIS

4.1 Introduction

The results obtained from the laboratory tests were analyzed using a Microsoft Excel™ spreadsheet that allowed an evaluation of the relationship between base properties and the resilient modulus. The effect of compaction and/or triaxial testing on the gradation of the sample was assessed after completing resilient modulus tests on a few test samples. Statistical analysis was conducted to develop models that would allow a more through estimation of the resilient modulus. Finally, a design table and a design chart of base properties were developed for Level 3 inputs.

4.2 Laboratory Test Results

To characterize the local base material properties, samples obtained from 14 locations were tested between December 2015 and December 2016. Three samples were not included in this analysis section: AGG. #1 and #2 were excluded due to insufficient quantity; AGG. #3 was excluded since it has a R-value less than the minimum value of 75 specified by WYDOT. The tests for M_r, R-value, modified Proctor test, plasticity index, liquid limits, and gradation were completed at the laboratory of WYDOT Materials & Testing Program in accordance with AASHTO test standards. WYODOT Materials & Testing Program reported the test results of the sample aggregates using WYODOT T-111, Rev. 7-95 form shown in Figure 4.1. The WYDOT test results of all aggregates at a disturbed condition are summarized in the master thesis entitled *Characterization of Crushed Base Materials in Wyoming* by Mebrahtom (2017).

4.3 Resilient Modulus (M_r)

The test procedure used to determine the resilient modulus of base materials was discussed in Section 3. The resilient moduli of all test specimens were determined separately by applying fifteen load sequences to each potential test sample prepared at four different moisture contents (one above optimum, two below optimum, and at optimum). However, AGG. #4 was prepared at two percent above optimum in addition to the four test specimens, and the five percent permanent deformation was attained during the test procedure. The sample was also too wet to handle. Therefore, testing at two percent above the optimum was excluded from all the samples testing procedure.

The output results of the ITC UniTest software were the actual axial load, the LVDT reading, resilient modulus of the last five pulses of each sequence, and the standard deviation and mean of the M_r. The pertinent information of the test sample was recorded in the sample worksheet prepared for base material as shown in Figure 3.7.

The controlling properties for the tests are summarized in Table 4.1. The measured dry density and moisture content displayed in Table 4.1 are slightly off the target values but within the AASHTO T 307 Type 1 moisture and density tolerances. The laboratory M_r value obtained from the UniTest software after finishing the 15 loading sequences are summarized in Tables 4.2 to 4.5, respectively. The average of the 15 M_r value was taken to indicate the laboratory M_r value of the sample aggregate at the respective moisture content as shown in Table 4.1. The resilient modulus test was not performed on AGG. #4 (Dry Creek Pit) at one percent above optimum because the sample was not sufficient for testing.

WYOMING DEPARTMENT OF TRANSPORTATION FORM T-111
MATERIALS TESTING LABORATORY REV. 7-95
REPORT OF TEST ON SOILS

LABORATORY
T-180

MAX DENSITY DRY	137.9	lbs/ft³
OPT MOISTURE	6.6	%

FIELD VALUES:

MAX DRY DENSITY		H₂O	%
FIELD DRY DEN.		H₂O	%
ROCK IN FILL			%
DENSITY TAKEN - DAY		AFTER FILL WAS PLACED	

CONSTRUCTION

LABORATORY NO	2016-0063		
FIELD IDENTIFICATION	U/W		
PROJECT NUMBER (S)	202014		
COUNTY	BIG HORN		
ENGINEER	MILLER		
ENGINEER TOWN	BASIN		
DATE SAMPLED	02/29/16	DATE REC'D	03/04/16
DATE TESTED	03/08/16	DATE POSTED	03/10/16

FIELD DATA:

SOURCE OF MATERIAL	DRY CREEK PIT (CB)
STATION SAMPLED	-
SECTION REPRESENTED	
DEPTH TAKEN	
VERTICAL LIMITS	

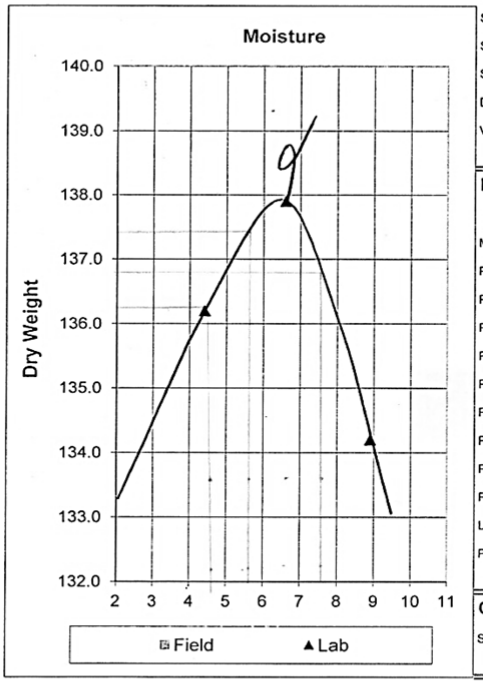

LABORATORY CONSTITUENT TESTS: *T-87, *T-88

MAX SIZE	
PAST NO. 50 mm (2")	%
PAST NO. 37.5 mm (1 1/2")	%
PAST NO. 25 mm (1")	%
PAST NO. 19 mm (3/4")	%
PAST NO. 9.5 mm (3/8")	%
PAST NO. 4.75 mm (#4)	%
PAST NO.2.00 mm (#10)	%
PAST NO. 425 µm (#40)	%
PAST NO. 75 µm (#200)	%
LIQUID LIMIT T-89	
PLASTIC INDEX T-90	

CLASSIFICATION:

SOIL TYPE & G.I. M-145

STABILOMETER: "R" VALUE T-190 76

*WYOMING MODIFIED

REMARKS

TESTED BY: MS,CM,DG,CI,JR,TG,RB
REVIEWED BY: J. DAGNILLO, P. E.

ASSISTANT STATE MATERIALS ENGINEER
MATERIALS ENGINEER

Y:\Soils & Surfacing\T 180 & T 99\0202014 DRY CREEK T-180 CB.xls Page 1

Figure 4.1 A sample WYDOT Rev. 7-95 form for an aggregate obtained from Pass Creek Pit

Table 4.1 Laboratory derived average resilient modulus values

AGG No.	Material Source	Opt. M.C (%)	γ_{max} (pcf)	Target M.C (%)	Measured M.C. (%)	Target γ_{dry} (pcf)	Measured γ_{dry} (pcf)	M_r (psi)
AGG-3* (Type-1)	Rieter Pit	6.8	135.7	4.8	5.0	134.3	130.3	36675
				5.8	5.8	135.5	134.3	33992
				6.8	7.19	135.7	134.0	28897
				7.8	7.6	134.8	133.7	25925
AGG-4 (Type-1)	Pass Creek Pit	6.1	141.1	4.1	4.0	139.2	135.3	36791
				5.1	5.2	140.5	135.6	33372
				6.1	6.4	141.1	141.5	22388
				7.1	7.3	140.0	138.2	23610
				8.1	8.0	138.0	137.1	21604
AGG-5 (Type-1)	Dry Creek Pit	6.6	137.9	4.6	4.8	136.3	128.6	33982
				5.6	5.8	137.4	132.2	32481
				6.6	6.6	137.9	135.4	29022
AGG-6 (Type-1)	Scarlett Pit	6	138.1	4	4.1	135.4	134.2	35799
				5	5.2	137.1	134.7	33986
				6	6.2	138.1	137.4	28479
				7	6.9	137.0	137.9	24191
AGG-7 (Type-1)	Simon's Pit	6.4	138.7	4.4	4.5	137.0	131.5	39166
				5.4	6.1	138.3	134.2	34460
				6.4	6.8	138.7	137.8	26826
				7.4	7.4	137.7	133.5	25052
AGG-8 (Type-1)	Eagle Creek Pit	6	142.9	4	4.3	140.8	136.8	47692
				5	4.6	142.6	138.3	43986
				6	6.2	142.9	141.1	41048
				7	7.0	141.8	140.7	35029
AGG-9 (Type-1)	Rogers Quarry Pit	6	140.7	4	4.3	139.2	135.7	43429
				5	5.6	140.6	139.1	44743
				6	5.8	140.7	138.4	42878
				7	6.6	139.5	138.4	35944
AGG-10 (Type-1)	VR Pit	6.1	141.7	4.1	4.2	135.9	134.0	37262
				5.1	5.0	139.9	136.4	35258
				6.1	6.5	141.7	139.8	29535
				7.1	7.1	141.2	141.6	22022
AGG-11 (Type-1)	Mullinax Pit	6.8	139.6	4.8	5.0	138.1	133.3	40746
				5.8	6.2	139.2	137.0	40012
				6.8	7.2	139.6	137.0	33370
				7.8	7.5	138.3	138.3	24685
AGG-12 (Type-1)	Gosney Pit	6.2	139.3	4.2	4.4	137.6	133.4	41664
				5.2	5.6	139.1	136.3	38514
				6.2	6.5	139.3	136.8	33647
				7.2	7.7	138.3	138.4	22528
AGG-13 (Type-1)	4 Mile Pit	6.2	140.7	4.2	4.7	139.2	130.9	42758
				5.2	5.6	140.6	136.3	37949
				6.2	6.3	140.7	136.2	40940
				7.2	7.0	139.5	136.9	32663
AGG-14 (Type-1)	Granite Canyon Quarry Pit	6.3	143.4	4.3	4.7	142.6	138.6	36726
				5.3	5.5	143.6	144.0	35655
				6.3	6.7	143.4	140.2	33839
				7.3	6.9	141.9	142.9	NA

AGG−Aggregate, *−Test results of AGG-3 were included for information only, Opt.−Optimum, γ_{max}−Maximum Dry Density, M.C.−Moisture Content, M_r−Resilient Modulus, and NA−Not available as the sample experienced a 5% deformation during the preconditioning stage.

Table 4.2 Average M_r at one percent above optimum for each load sequence

AGG. #	M_r value at Each Load Sequence (psi)														
	1	2	3	4	5	6	7	8	9	10	11	12	13	14	15
4	7779	10161	12260	12747	15609	17385	22663	25745	27045	26799	28993	33854	35125	37311	40671
5	NA	NA	NA	NA	NA	NA	NA	NA	NA	NA	NA	NA	NA	NA	NA
6	9269	11031	12878	13694	16335	18128	23471	26593	27604	27836	29099	33507	35266	36659	41494
7	8835	11296	12906	13622	16376	18290	23743	26958	28657	29232	30946	35761	37182	39183	42794
8	14882	17767	20564	20971	25065	28696	35212	39914	40083	42270	43258	46716	49708	50656	49668
9	15491	17960	20049	20856	24673	28339	35244	40052	42278	42519	44794	48406	52038	53077	53382
10	8063	10411	12667	11663	14831	17923	20203	24449	27149	24066	25979	31153	31355	33043	37381
11	10602	13333	15781	13367	17673	20682	20086	25525	28206	21840	24784	30682	28040	30615	36702
12	10069	15280	18507	17932	22625	26945	32099	37678	39701	39599	40224	45337	47025	47749	49170
13	8870	12096	15112	12416	17594	20766	22568	27893	30875	26317	28430	35000	34078	37357	40897

Table 4.3 Average M_r at optimum for each load sequence

AGG. #	M_r value at Each Load Sequence (psi)														
	1	2	3	4	5	6	7	8	9	10	11	12	13	14	15
4	7389	10395	12641	10822	14771	17723	19837	24416	27462	24598	27036	32465	32430	35343	38485
5	12020	13705	15906	17248	20519	23502	28858	32776	33598	32947	35366	39811	40900	42868	45308
6	11767	13429	15587	16780	19542	22114	27316	31813	33593	32752	34423	39358	40468	41693	46548
7	9613	12421	14475	15522	18365	20296	26094	29224	30829	30939	32723	37477	38952	40824	44630
8	17939	20618	23640	24447	28985	34031	41998	46512	47408	50657	51151	52338	58092	59320	58585
9	18993	22090	24929	25937	31130	35026	42796	48913	50774	51177	52526	55844	60360	61041	61628
10	11738	14390	16831	17495	21249	24093	28866	33310	34845	33258	35293	40725	41734	43128	46072
11	14543	16703	19462	20422	24645	27579	33410	38387	39857	38593	40939	45189	46671	48432	49868
12	17306	18689	20990	23437	27114	30922	41135	45849	48913	51097	51765	55363	57925	60332	63257
13	9960	15291	17878	19036	22722	26340	32210	37526	40758	39236	41603	46947	48287	50382	52369
14	NA	16223	18231	15467	22837	26016	31836	36836	39045	37242	40007	44826	45837	48029	51319

Table 4.4 Average M_r at one percent below optimum for each load sequence

AGG. #	M_r value at Each Load Sequence (psi)														
	1	2	3	4	5	6	7	8	9	10	11	12	13	14	15
4	10899	15732	17602	19576	22792	25538	32967	37010	40517	40080	42648	48282	40548	51890	54505
5	7552	15731	17989	18560	22955	25842	31676	37520	38954	37006	40369	45698	46489	48791	52086
6	14072	16082	18660	19755	23384	26144	33106	38208	40539	40696	41652	46701	48313	49230	53244
7	14555	16661	18678	19956	23940	27077	34229	39208	41400	40438	42855	46615	48439	50291	52554
8	21310	23824	26658	28825	32778	36889	45874	48501	50096	52630	53876	53274	58993	61768	64500
9	22119	24620	27938	29357	35562	37876	45842	49842	52752	52500	54160	57087	59062	60623	61800
10	12315	16544	18716	19827	23766	27040	33557	39590	43406	40443	43831	50366	50542	52113	56813
11	NA	18571	19770	20500	NA	28376	34498	40618	43081	40820	45114	50047	51406	53383	54503
12	NA	15557	18094	16520	23116	27054	34943	39989	42908	45526	46308	50455	54358	55498	60955
13	17685	19151	21487	23487	27233	30552	39680	44957	47680	49368	49939	54967	56464	57556	59974
14	14850	16894	19493	21200	24936	27835	35099	40710	42449	41718	44030	48997	49956	52296	54367

Table 4.5 Average M_r at two percent below optimum for each load sequence

AGG. #	M_r value at Each Load Sequence (psi)														
	1	2	3	4	5	6	7	8	9	10	11	12	13	14	15
4	16336	18598	20982	22207	25948	29114	35914	41549	43879	42568	45661	49973	50586	53307	55243
5	13492	16786	18674	19960	23368	26090	33180	37450	40015	39553	42101	47245	48146	50322	53345
6	13830	16522	19002	20314	24231	27581	35000	39831	42415	42083	44425	50116	51150	55018	55462
7	18667	20250	22044	23811	27160	30095	37213	43275	45783	45452	47661	53373	54846	58339	59524
8	21003	23292	26558	28999	33295	37453	47333	51476	55116	57728	60420	64140	68868	67914	71783
9	NA	20348	23340	20831	29210	33718	42535	47668	49094	49752	51851	55540	59590	61549	62974
10	NA	17185	19171	NA	23768	26244	33608	37966	40422	40554	43045	46892	49532	51905	54120
11	19248	20755	22696	25181	28463	31917	41023	46801	49314	50034	51951	54519	58591	59068	65396
12	14259	20567	22366	25243	28124	31580	40680	46800	50408	53052	53668	59236	63430	64834	67127
13	18352	19662	21748	24216	27048	30503	38834	45510	47869	51126	50564	54969	60310	59085	61400
14	15534	17583	19764	21418	24970	28611	35808	40746	43515	43212	46240	49638	52650	54703	56503

4.4 Gradation Check

Sieve analysis was performed in according with AASHTO T 88 to determine the gradations of the base sample from Simons Pit before and after the M_r testing. Comparison of the gradations was done to evaluate if a change occurred in aggregate shape or gradation after compaction and M_r testing. The sieve analysis was performed by disintegrating the sample when it was wet, followed by oven drying, and then sieving. This sample prepared at the optimum moisture content shows a negligibly change in gradation (see Table 4.6). Therefore, the possible effect of compaction and M_r triaxial loading test on the change in gradation was not observed in this study.

Table 4.6 Gradation comparison of a base sample from Simons Pit

Sieve Size (in)	Simons Pit at Optimum M.C	
	Percent Passing before M_r Test	Percent Passing after M_r Test
¾"	93	93.8
½"	75	76.1
⅜"	68	68.0
#4	57	57.1
- #4	50	49.1

M.C.−Moisture content, #4–No. 4 sieve size, and -#4–Below No. 4 sieve size.

The resilient modulus tests were completed on 11 samples at five confining pressures of 3 psi, 5 psi, 10 psi, 15 psi and 20 psi. The analyses of stress, moisture, density, percent fines, and gradation were done using Microsoft Excel™ and statistic software known as R-program. The summarized resilient modulus recorded worksheet can be found in the thesis by Mebrahtom (2017) thesis. The average M_r output results of the last five pulses of each load sequence at four different moisture contents are summarized in Tables 4.2 to Table 4.5, respectively.

In Sections 4.4.1 to 4.4.4, the effect of the influential predictors to the resilient modulus was addressed using the laboratory-measured data. Since the MEPDG software requires M_r value at optimum moisture content, the analysis of the influential predictors to M_r was conducted using the data displayed in Table 4.3. The effect of moisture content to M_r was assessed using the other data shown in Tables 4.2 to Table 4.5.

4.4.1 Confining, Axial, and Bulk Stress

In this study, the effect of both axial and confining stresses, in according to the test sequences in Table 2.4, was analyzed. At a lower axial stress level (i.e., less than 15 psi) and a lower confining stress level (3 and 5 psi), the M_r value increases with the increase in axial and confining stresses. However, at a higher axial stress level (i.e., greater than 15 psi) and a higher confining stress level (10, 15 and 20 psi), the effect of confining stress on M_r is more significant than that based on the axial stress. For example, the effect of stresses on the M_r values of aggregate at optimum from Pass Creek Pit is shown in Figure 4.2. At a higher stress level, an increase of 5 psi (from 10 to 15 psi) in confining stress at a constant axial stress of 30 psi increased the resilient modulus by 18 percent. At a constant confining stress of 10 psi, the increase in axial stress from 10 to 30 psi increased the resilient modulus by 38 percent. For the lower stress level, an increase of confining stress by 2 psi (from 3 to 5 psi) and an increase of axial stress by 1 psi (from 9 to

10 psi) increased the resilient modulus by 17 percent. However, the increase of axial stress by 3 psi (from 3 to 6 psi) and 6 psi (from 3 to 9 psi) at a constant confining stress of 3 psi increased the resilient modulus by 41 percent and 71 percent, respectively.

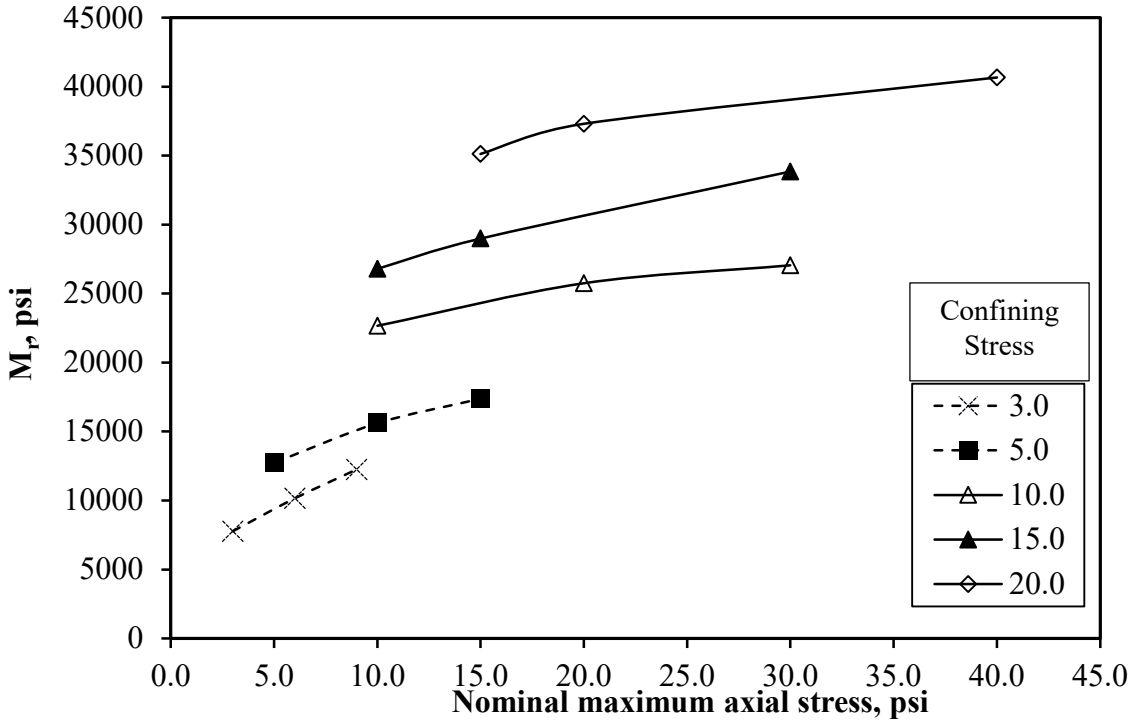

Figure 4.2 Stresses on resilient modulus for aggregates obtained from Pass Creek Pit at optimum moisture content

Summaries of test results of all samples was prepared to better understand the effect of confining and axial stresses at the lower and upper stress levels on M_r value. Table 4.7 shows the percent increase in resilient modulus at 50 percent increase in confining stress and 200 percent increase in axial stress. The percent increase in M_r due to 200 percent increase in axial stress and 50 percent increase in confining stress are quite similar except aggregate No. 4. Hence, it can be concluded that at the upper stress level, the effect of confining stress is more significant than the axial stress.

Table 4.7 Effect of confining and axial stresses to M_r at upper stress level

Higher Level of Axial and Confining stresses	**Percent increase in M_r for Aggregate No.**										
	4	5	6	7	8	9	10	11	12	13	14
50 percent increase in confining stress at 30 psi constant axial stress	18	18	17	22	10	10	17	13	13	15	15
200 percent increase in axial at 10 psi constant confining pressure	38	16	23	18	13	19	21	19	19	27	23

M_r −Resilient Modulus, confining stress was taken from sequences 9 and 12 (10 to 15 psi), and Nominal Maximum Axial Stress was taken from sequences 7 and 9 (10 to 30 psi).

Table 4.8 summarizes the percent increase in M_r values at three lower stress conditions for aggregates 4 to 12. Results of aggregates No.13 and No.14 were not included because the percent increase in the resilient modulus seemed to be an outlier for aggregate No. 13. Also, test data for aggregate No. 14 at 3 psi confining stress was not recorded possibly due to the gap between the loading piston and specimen. The

percent increase in M_r, due to a 100 percent increase in axial stress, is less than that based on 67 percent increase in confining stress, and an 11 percent increase in axial stress, except for aggregates No. 4 and No. 7. The percent increase in M_r due to 200 percent increase in axial stress, percent increase in M_r at 67 percent increase in confining, and 11 percent increase in axial stress, are similar, except aggregates No. 4, No. 7, and No. 10. Similarly, the influence of the confining stress was found to be more significant at the lower stress levels. Hence, confining stress has a greater influence at both lower and higher stress levels.

Table 4.8 Effect of confining and axial to M_r at lower stress level

Lower Level of Axial and Confining stresses	**Percent increase in M_r for Aggregate No.**								
	4	5	6	7	8	9	10	11	12
100 percent increase in axial stress at a constant 3 psi confining stress	41	14	14	29	15	16	23	15	8
200 percent increase in axial stress at a constant 3 psi confining stress	71	32	32	51	32	31	43	34	21
67 percent increase in confining stress and 11 percent increase in axial stress	17	29	25	27	23	25	26	27	29

Although the effect of axial stress at both lower and upper stress levels was found to be lower than confining stress, its influence on the determination of M_r value cannot be neglected. Therefore, researchers (see Section 2.3.1.1) used the sum of principal stresses to account for the effect of both confining and axial stresses.

In this study, the effect of bulk stress to M_r was also examined. The laboratory measured average M_r values of the 11 samples tested at optimum moisture content are compared with bulk stress in Figure 4.3. A linear positive relationship was found between bulk stress and M_r with a relatively high coefficient of determination (R^2) of 0.9755. Furthermore, results of individual aggregate sample show the same relationship between bulk stress and resilient modulus (Mebrahtom 2017). Therefore, the constitutive model developed by Hicks and Monismith (1971) was used for calibration in this study.

4.4.2 Moisture Content

To analyze the impact of moisture on the resilient modulus, aggregate No. 4 was initially prepared at five different moisture contents. Two samples were prepared with moisture contents above optimum moisture, one sample at optimum, and two samples below optimum. However, the sample at two percent above the optimum moisture content was too wet for handling, compaction, and achieving the target dry density (see Figure 4.4). This sample was twisted during the M_r testing and experienced the five percent permanent deformation that was noticed at the end of the M_r testing. Therefore, all samples were prepared at four moisture contents excluding the moisture content at two percent above the optimum.

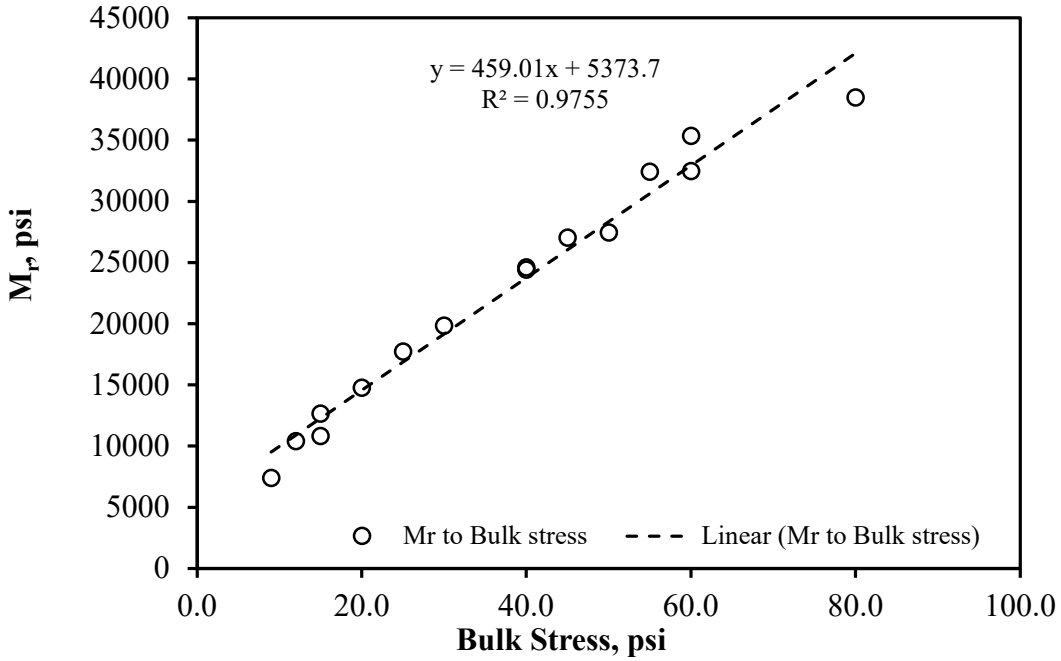

Figure 4.3 Relationship between bulk stress and M_r for aggregate samples tested at optimum moisture content

To evaluate the impact of moisture content on the M_r value, the samples were classified according to WYDOT grading system. Figure 4.5 and Figure 4.6 show the relationships between moisture content and M_r value for "L" and "W" grading samples, respectively. Figure 4.5 shows that the resilient modulus of Rogers Quarry Pit (AGG-9) shows an initial increase in M_r from two percent below to one percent below optimum moisture content, and the M_r decreases as the moisture increases. The M_r values of both sample aggregates from Eagle Creek Pit (AGG-8) and Granite Canyon quarry (AGG-14) decrease with increasing moisture content. Among these three aggregates, the measured M_r values of AGG-14 were relatively lower than that of AGG-8 and AGG-9. This could be attributed to the geology of AGG-14 that was not identified as limestone. In addition, this observation aligns with the relatively low R-value of 76 for AGG-14 compared with 88 and 79 for AGG-8 and AGG-9, respectively. Generally, it can be concluded that the M_r of base samples with L-grading decreases with increasing moisture content.

The relationships between moisture content and M_r for W-grading base materials are shown in Figure 4.6. The results reveal that the M_r value was also inversely proportional to the moisture content. Particularly, aggregates from Mullinax, Dry Creek, Scarlette, VR, and Simon's Pit show a gradual decrease in M_r as the moisture content increases from two percent below optimum to one percent above optimum. The moisture content was found to be highly significant to the decrease in resilient modulus at both W and L grading base materials in Wyoming.

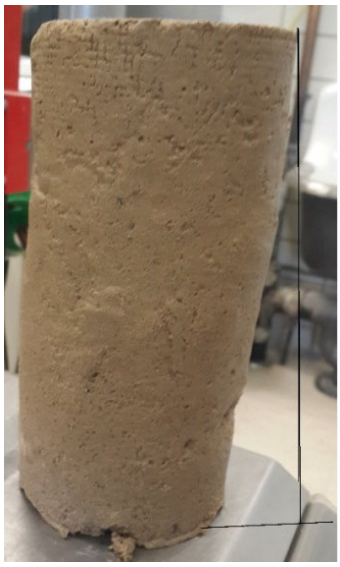

Figure 4.4 Rejected aggregate from Pass Creek Pit compacted at two percent above optimum

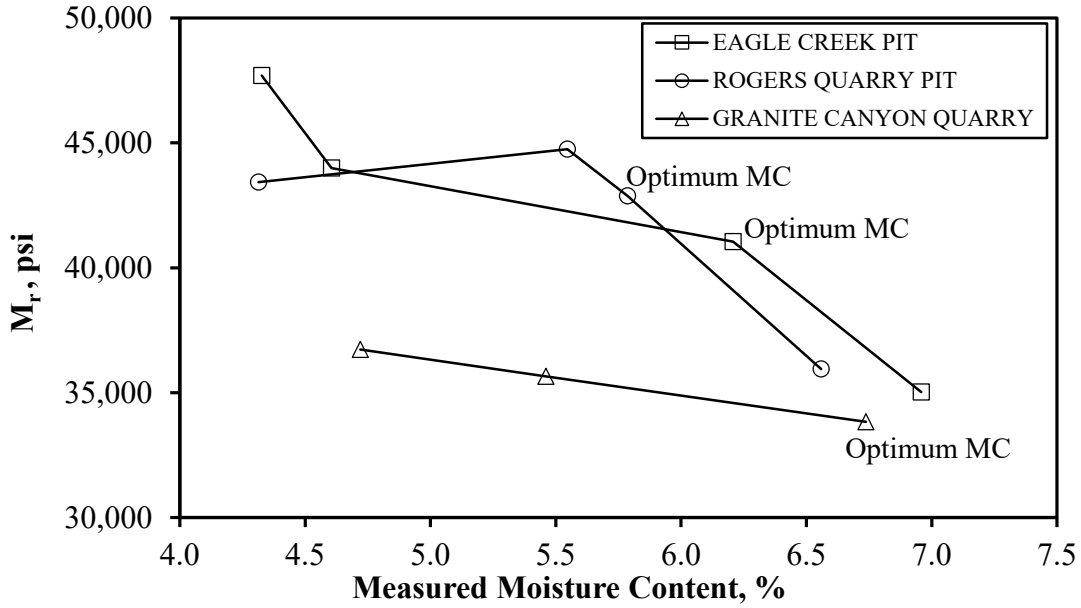

Figure 4.5 Relationship between moisture content and M_r value for L-grading base materials

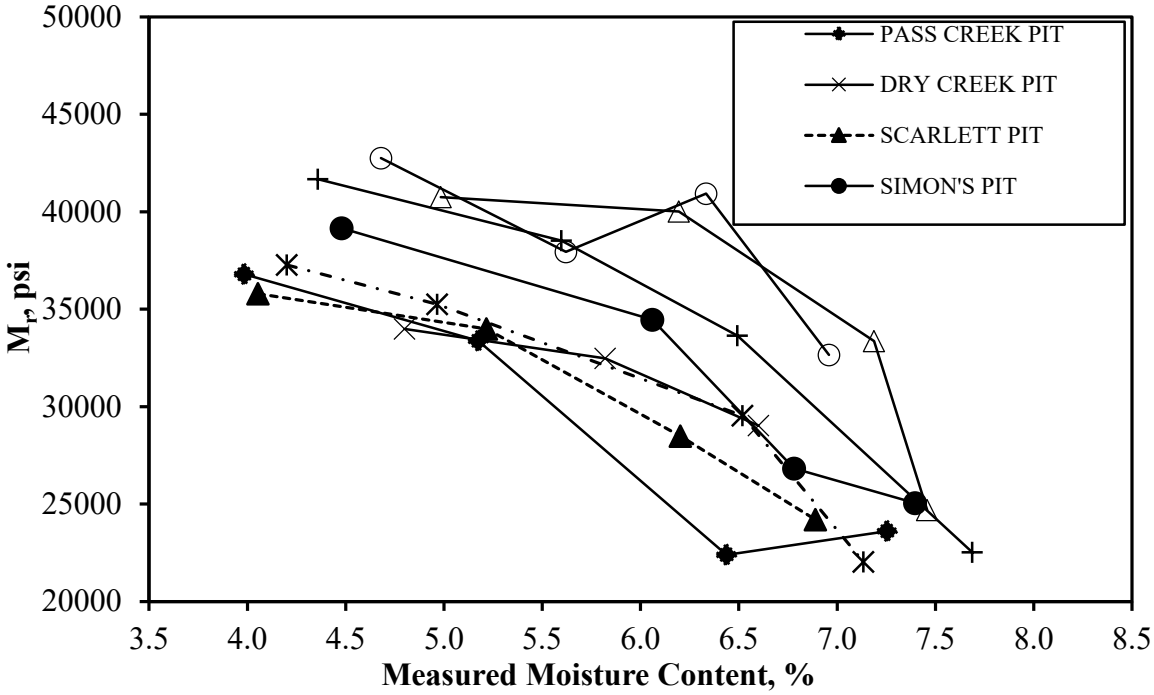

Figure 4.6 Relationship between moisture content and M_r value for W-grading base materials

4.4.3 Density

The limiting target density, according to AASHTO T 307 protocol for the Type 1 untreated base/subbase material, shall be within ±3 percent of the maximum dry density. Figure 4.7 shows the relationship between the measured maximum dry density and the M_r value of tested samples at optimum moisture content. Figure 4.7 shows that the effect of density on the resilient modulus cannot be clearly determined because of the narrow range of maximum dry density used in this study (between 135 to 144 pcf). Similar observation was noted for base samples at below and above optimum moisture contents (Mebrahtom 2017).

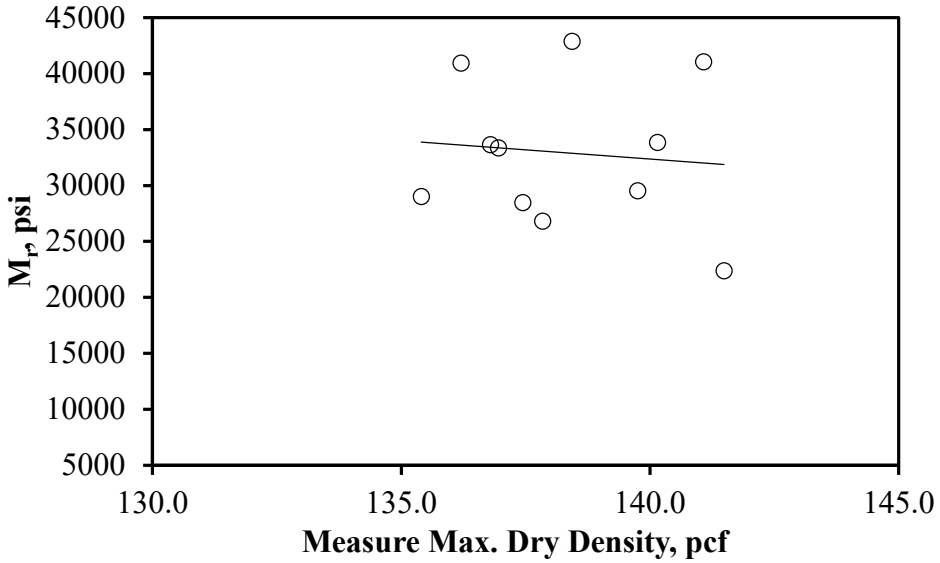

Figure 4.7 Influence of maximum dry density on the M_r of base materials

4.4.4 Percent Fines

The range of percent fines for the W and L-grading base materials is between 3 and 12 percent in according with the WYDOT specification Table 803.4.4.-1 (2010). In this study, the percent fines were determined ranging from 5.9 to 11.9 percent, and the samples were categorized according to their target moisture content test levels. Figures 4.8 through 4.11 show no relationship between percent fines and resilient modulus of base samples at four moisture contents. This outcome could be attributed to the narrow range of percent fines considered in this study.

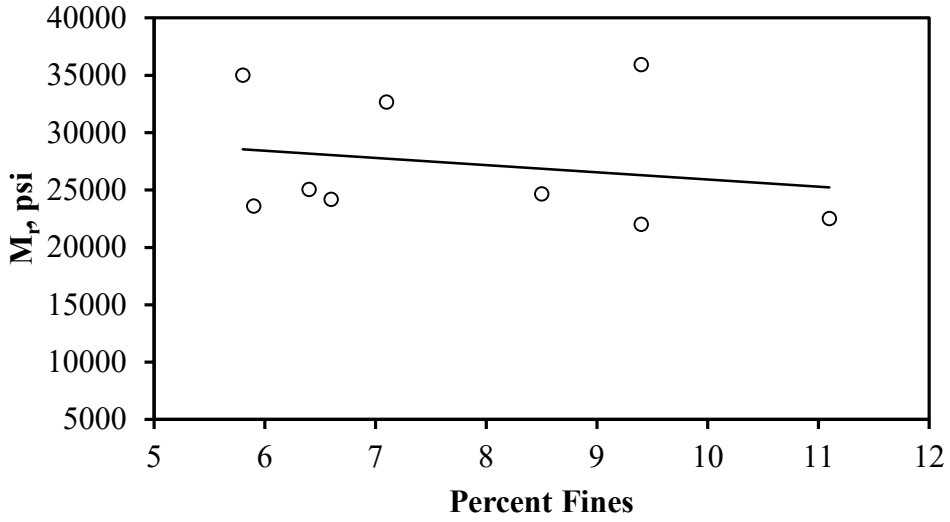

Figure 4.8 Effect of percent fines on M_r of base samples at one percent above optimum

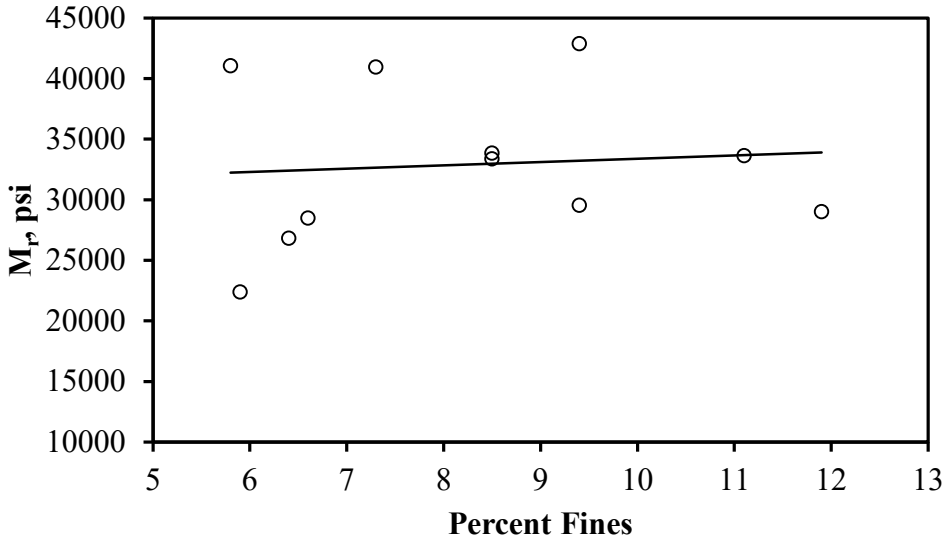

Figure 4.9 Effect of percent fines on M_r of base samples at optimum

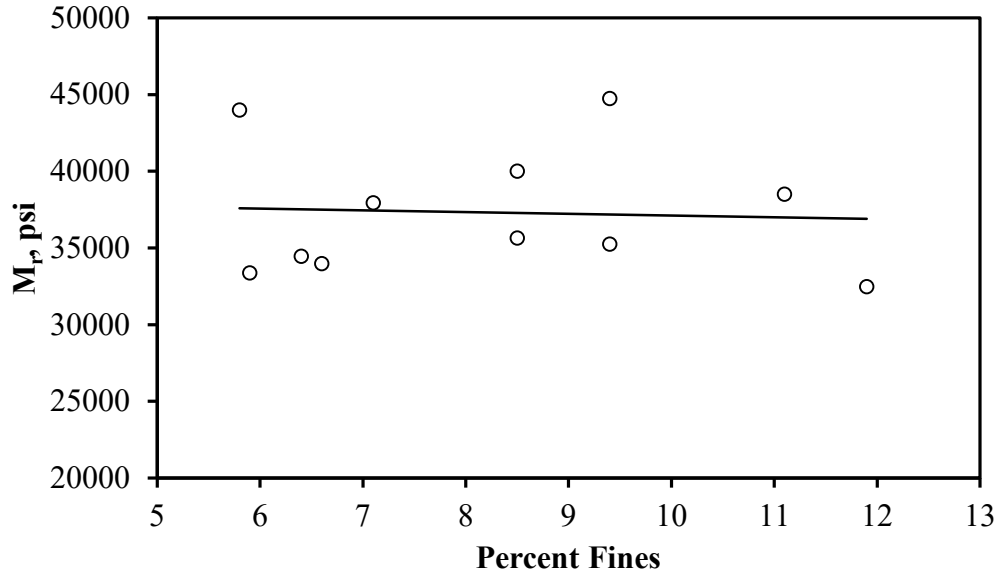

Figure 4.10 Effect of percent fines on M_r of base samples at one percent below optimum

The effect of aggregate shape, rock type, and particle size on the resilient modulus was not considered in this research, because round aggregates (pit run) were combined with crushed aggregates (crushed run), limited rock types were tested, and the use of a 4-in mold size restricted the testing on the three fourth nominal maximum aggregate size.

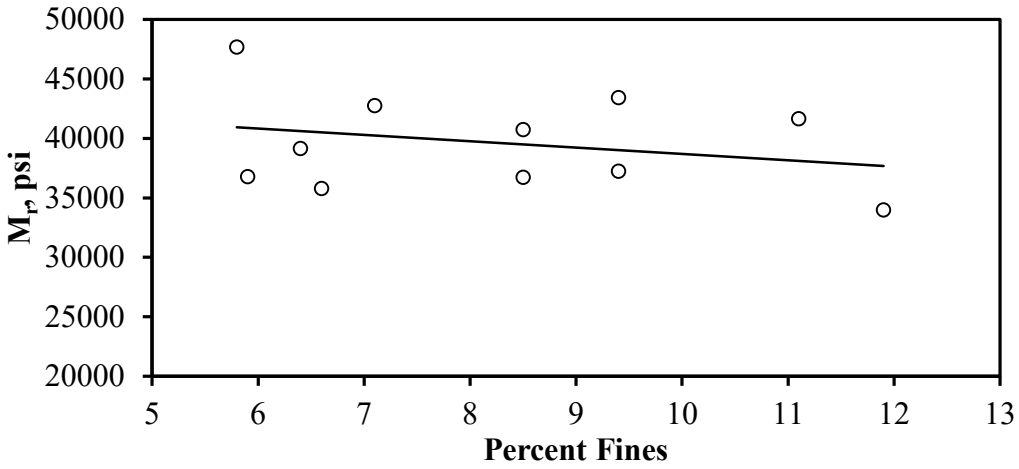

Figure 4.11 Effect of percent fines on M_r of base samples at two percent below optimum

4.5 Fractured Aggregate Face

A statistical analysis was conducted to determine the influence of the one fractured face of the aggregates on the M_r value. In this study, eight aggregates of the 11 sources have one fractured face (Table 3.2), and the percent of one fractured face ranges from 83 to 100, indicating all the aggregates have similar one fractured face. According to the WYDOT gradation, the L-grading aggregates (Eagle Creek Pit, Rogers Quarry Pit, and Granite Canyon Quarry Pit) have 100 percent one fractured face, and the W-grading samples (Dry Creek Pit, VR Pit, Mullinax Pit, and 4 Mile Pit) have 83 to 90 percent one fractured face. This relatively high percentage shows that the range of fractured face does not include the lower percentage of one fractured face. According to WYDOT specification 817.0 (2012), base aggregates

should have one fractured face of 50 percent or greater. Figure 4.12 shows no relationship between percent of one fractured face and M_r value at optimum moisture condition. Figure 4.13 again shows no relationship between R-value and percent of one fractured face. Same observation of having no relationship between R-value and percent of one fractured face was noted for samples at below and above optimum moisture conditions (Mebrahtom 2017).

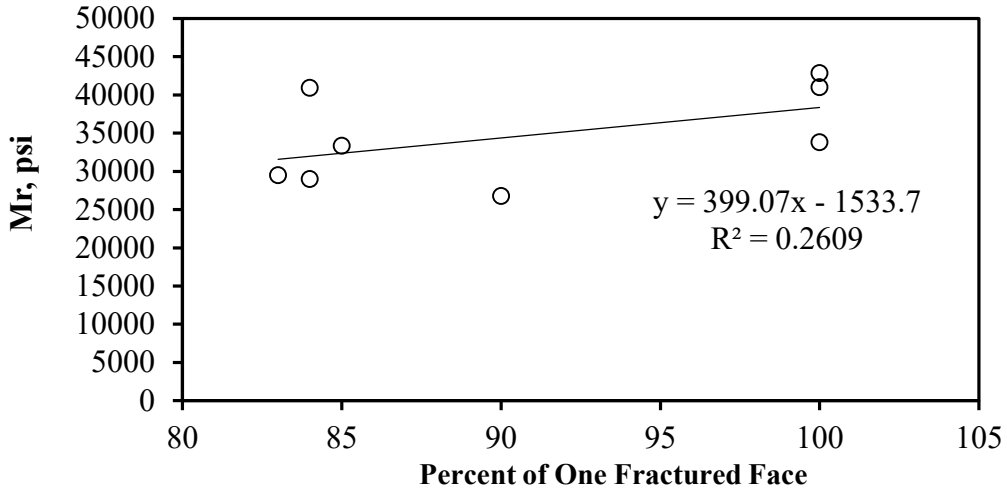

Figure 4.12 Average M_r versus percent of one fractured face of samples at optimum moisture content

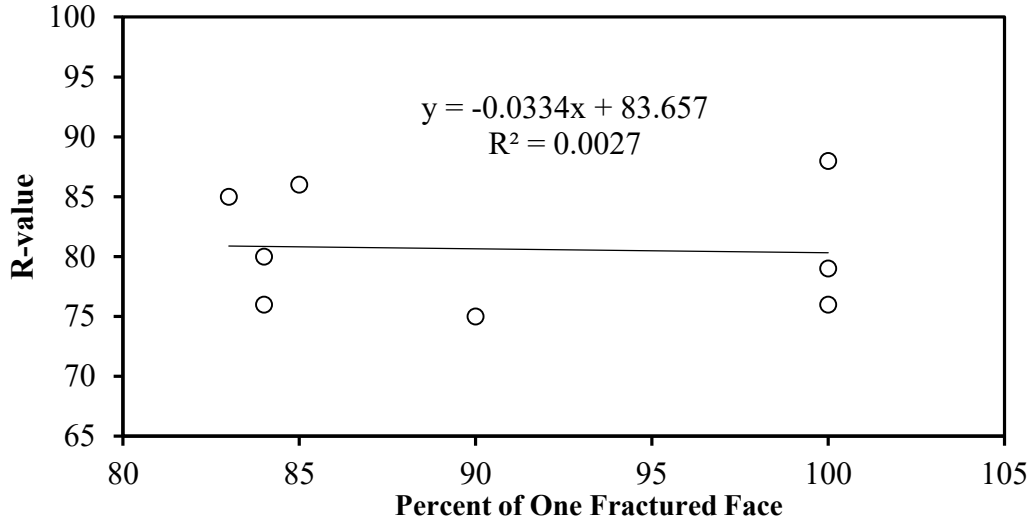

Figure 4.13 R-value versus percent of one fractured face of samples at optimum moisture content

4.6 Correlation between R-value and M_r -value

The R-value is commonly used by the WYDOT and other state DOTs for characterizing base materials used in the design of flexible pavements. The R-value equipment and method of testing are readily available to most DOTs, while resilient modulus testing machines are expensive as sample preparation and testing can be time consuming and tedious. Therefore, a correlation of the R-value and the M_r-value could be beneficial for a pavement design.

In this study, the direct correlation between R-value and resilient modulus was attempted at four target moisture contents. As an example, correlation between M_r and the R-value of base samples at optimum moisture content is shown in Figure 4.14, with a relatively low coefficient of determination ($R^2 = 0.176$). Therefore, a direct relationship between M_r and R-value was not determined to yield an accurate estimation of M_r. Statistical analyses were also conducted between R-value and M_r value of base samples at below and above optimum moisture content conditions, and poor correlations were found (Mebrahtom 2017). This could be due to a small sample size and all R-values greater than 75. Even though no direct correlation was obtained between R-value and M_r value, R-value was found to be significant in predicting the M_r value when other predictors were added as discussed in Section 4.7.2.

4.7 Statistical Analysis

Statistical analysis was helpful in identifying significant parameters for developing M_r model in this study. A simple linear regression analysis was conducted to determine the influential predictors of M_r, and multiple regression analysis was used for the resilient modulus estimation in the presence of multiple predictors. The linear and nonlinear regression models were only applied to the simple Hicks and Monismith (1971) model given by Equation (2.3), and the NCHRP model given by Equation (2.7) in Section 2.7. The simple Hicks and Monismith (1971) model relates the resilient modulus with the highly significant predictor bulk stress. The NCHRP (2004) model, adopted in AASHTO Ware pavement ME-design software, relates both the bulk stress and octahedral shear stress to the resilient modulus.

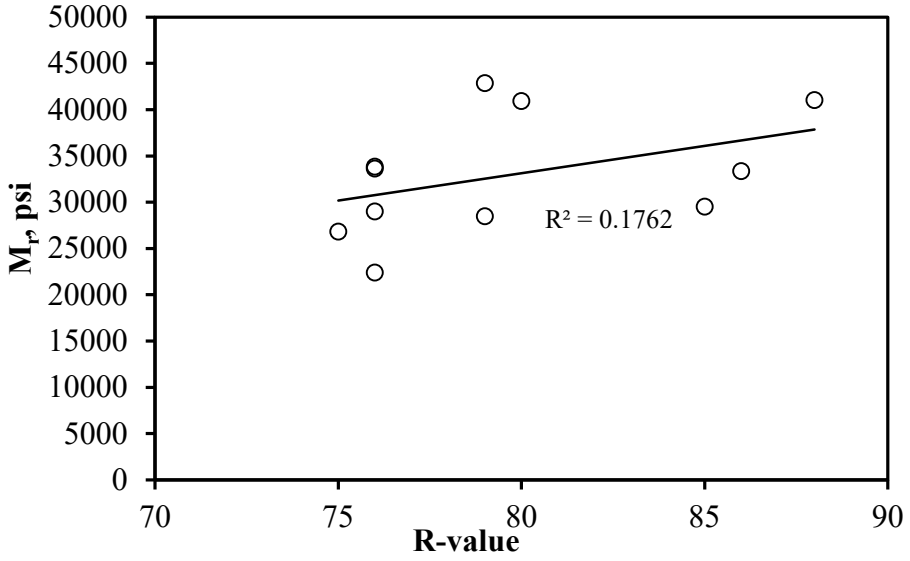

Figure 4.14 Correlation of R-value and M_r of base samples at optimum moisture content

4.7.1 Simple Linear regression analysis (SLR)

The linear association of the influential predictors to the resilient modulus was evaluated using a significance level of 0.05. The t-test was conducted for testing the null hypothesis (H_o:$\beta_1 = 0$, the slope of the linear model is zero), and the alternative hypothesis (H_a:$\beta_1 \neq 0$, the slope of the linear model is not zero). To conclude whether the null hypothesis or the alternative is accepted, the P-value obtained from the t-test (p-value) was compared with the chosen significance level. If p-value is greater than the significance level, no linear association is declared between the predictor and resilient modulus at that significance level. If p-value is less than the significance level, there is a linear association between the predictor and the resilient modulus is declared.

The t-test results for the simple linear regression model between M_r and each of the predictor is shown in Table 4.9. The significance level specified earlier was compared with the P-value obtained from the t-test. A linear relationship was not found between M_r and each of the other stated predictors except the grading and bulk stress. The linear regression assumption (linearity, consistency, normality, outlier and lack of fit) were also considered in the analysis. Since there was not a time dependent or sequential sampling method, the residuals were assumed to be independent.

Table 4.9 Estimated SLR models for resilient modulus

Predictor and corresponded Intercept	Estimate	Std. Error	t value	P-value	Sigmah	cov	R^2
Intercept (ω_{opt})	82837	34682	2.388	0.0407	6197.759	18.834	0.188
ω_{opt}	-7714	5350	-1.442	0.183			
Intercept (γ_{dry})	77440.2	146452.9	0.529	0.61	6841.269	20.790	0.0102
γ_{dry}	-321.9	1058.6	-0.304	0.768			
Intercept (Percent fines)	30675.4	8888.9	3.451	0.007	6851.026	20.820	0.0073
Percent Fines	270.3	1047.4	0.258	0.802			
Intercept (R-value)	-14172.6	33985	-0.417	0.686	6241.205	18.966	0.176
R-value	591.2	426.1	1.387	0.199			
Intercept (Grading)	39255	3099	12.667	4.85E-07	5367.658	16.312	0.391
Grading	-8729	3634	-2.402	0.0398			
Intercept (Bulk Stress)	8896.25	1230.15	7.232	6.63e-06	2311.01	8.465	0.958
Bulk Stress	496.57	29.02	17.11	2.69e-10			

Estimate−Coefficient of the predictor or corresponded intercept, Std.–Standard Error, Sigmah–Estimated standard deviation, cov–Coefficient of variance, R^2 –Coefficient of determination, ω_{opt}–Pptimum moisture content, and γ_{dry}–Maximum Dry density.

4.7.2 Multiple Regression Analysis

Multiple regression analysis was chosen to account for the joint effects of the predictors (moisture content at optimum, maximum dry density, percent fines, R-value, and grading) on the M_r. Model assumptions of normality and consistency were checked using the Shapiro-Wilk test and Breush-Pagan test at a significance level of 0.05. The Shapiro-Wilk test checks whether the model errors are normally distributed, and the Bruesch-Pagan test checks whether the model errors have equal variance. Lack of fit due to interaction and quadratic terms were also checked using the analysis of variance. The pairwise scatter plot shown in Figure 4.15 was prepared to examine the relationship between the predictors and M_r. The pairwise scatter plot shows the correlation strength and direction among the predictors. The corresponding matrix of correlation coefficients is summarized in Table 4.10. The optimum moisture content (ω_{opt}) with a coefficient of -0.43 and the grading of the materials with a coefficient of -0.63 are negatively related to the resilient modulus with a relatively medium to strong correlation. R-value with a coefficient of 0.42 is positively related to resilient modulus with a relatively medium correlation strength. However, relatively poor correlation was observed between maximum dry density and M_r as well as between percent fines and M_r. Maximum dry density (γ_{dry}) has a negative and moderate autocorrelation with percent fines (coefficient of -0.54) and aggregate grading (coefficient of -0.49).

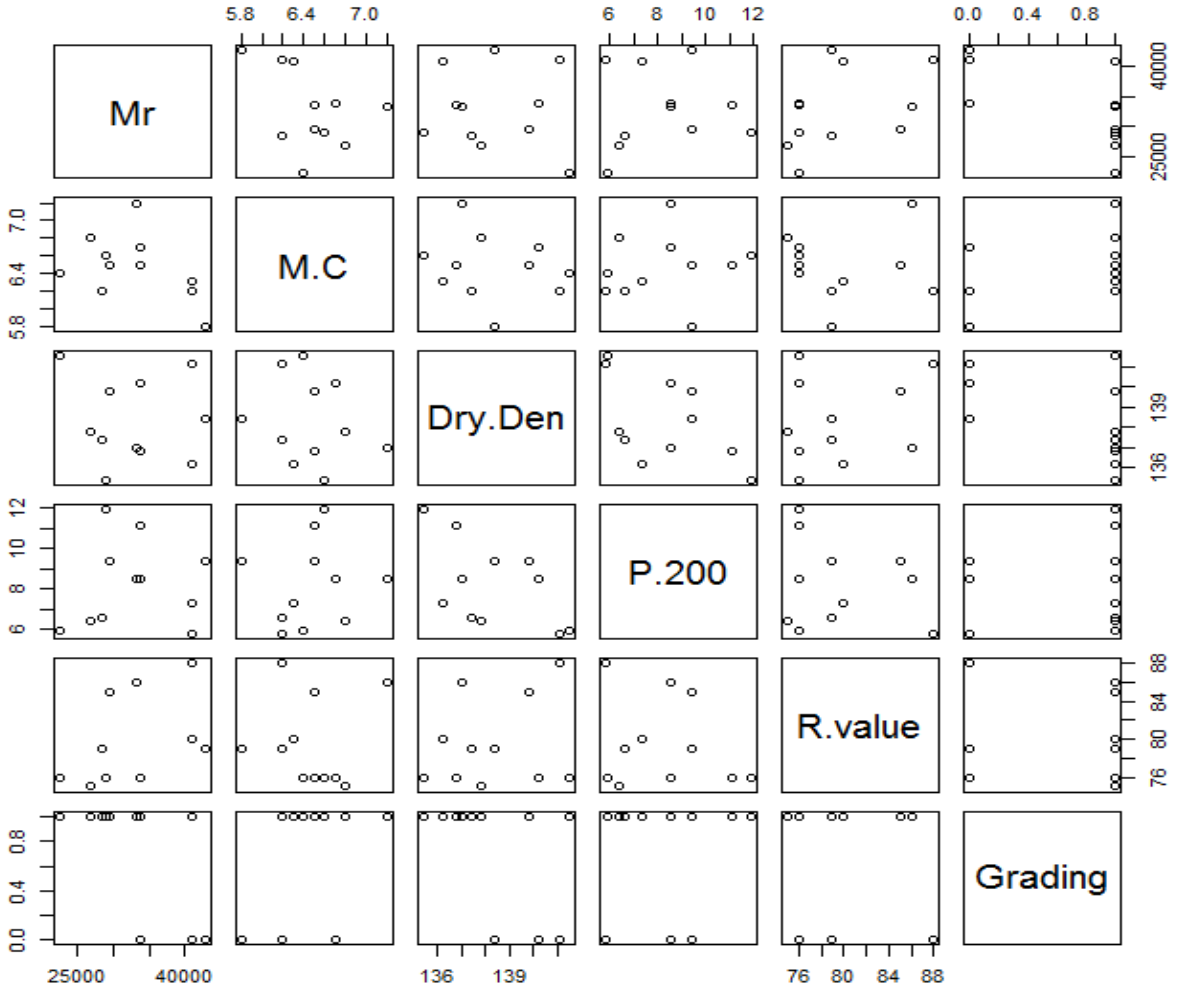

Mr−Resilient Modulus, M.C−Moisture Content, Dry Den.−Dry Density, P.200−Percent fine (passing # 200 sieve), R.value−R-value obtained using a stabilometer , and Grading−W or L grading.

Figure 4.15 Pairwise scatter plot of the predictors and resilient modulus at optimum moisture content

Table 4.10 Matrix of correlation coefficients

Predictors	M_r	ω_{opt}	γ_{dry}	Percent Fines	R-value	Grading
M_r	1.00	-0.43	-0.10	0.09	0.42	-0.63
ω_{opt}	n/a	1.00	-0.20	0.12	0.02	0.42
γ_{dry}	n/a	n/a	1.00	-0.54	0.24	-0.49
Percent Fines	n/a	n/a	n/a	1.00	-0.21	0.11
R-value	n/a	n/a	n/a	n/a	1.00	-0.19
Grading	n/a	n/a	n/a	n/a	n/a	1.00

M_r–Resilient modulus, ω_{opt} –Optimum moisture content, γ_{dry} –Maximum dry density, and n/a−Not applicable.

Multiple linear regression was used to establish a prediction model of resilient modulus. The resilient modulus measured at optimum moisture content and the measured predictors used in the multiple regression analysis are summarized in Table 4.11.

Table 4.11 Summary of influential predictors and averaged M_r value

AGG. #	M_r, psi	Optimum Moisture Content (percent)	Maximum Dry Density (pcf)	Percent Passing No. 200 Sieve	R-value	WYDOT Grading
4	22388	6.4	141.5	5.9	76	1
5	29022	6.6	135.4	11.9	76	1
6	28479	6.2	137.4	6.6	79	1
7	26826	6.8	137.8	6.4	75	1
8	41048	6.2	141.1	5.8	88	0
9	42878	5.8	138.4	9.4	79	0
10	29535	6.5	139.8	9.4	85	1
11	33370	7.2	137	8.5	86	1
12	33647	6.5	136.8	11.1	76	1
13	40940	6.3	136.2	7.3	80	1
14	33839	6.7	140.2	8.5	76	0

AGG. #−Aggregate number, M_r −Resilient Modulus, and WYDOT grading−"1" for W grading and "0" for L grading.

The iterative process was done by eliminating non-significant predictors with p-value greater than 0.05. All the predictors were found to be non-significant except the grading. Practically, predicting the resilient modulus using the grading only might be unrealistic. Therefore, to include other predictors, a higher p-value of 0.1 was adopted in this study. The t-test outputs for the final prediction representative M_r value model is summarized in Table 4.12, and the prediction model for M_r is given by Equation (4.1). The total sum of error square of the estimated model is 98,731,079, and the adjusted R-square is equal to 0.67.

Table 4.12 Regression coefficient estimates for prediction model with significant level of 0.1

Term	Estimates	Std. Error	t-value	P-value
Intercept	270224.8	93695.2	2.884	0.02351
γ_{dry}	-1982.9	678.6	-2.922	0.02227
R-value	573.4	265	2.163	0.06728
Grading	-11942.2	2935.1	-4.069	0.00476

$$\widehat{M}_r = 270224.8 - 1982.9(\gamma_{dry}) + 573.4(R) - 11942.2(Grading) \quad (4.1)$$

where,

$\widehat{M}_r$= estimated resilient modulus at optimum moisture content (psi),
γ_{dry} = maximum dry density (pcf),
R = R-value determined from T-190 test at 300 psi exudation pressure, and
Grading = "1" for W-grading and "0" for L-grading.

Best subset selection method was used to select a best model using the criteria adjusted R-square, Akaike's information criteria (AIC), Schwarz' Bayesian criteria (BIC), and Mallows' criterion (C_p). The adjusted R-square criterion penalizes for the number of parameters and explains the total variation of the estimated values accounted for by the model. The best model has the highest adjusted R-square. AIC and BIC penalize for adding predictors, and best model selection is done based on the smallest AIC or BIC value. The criterion for C_p considers the mean squared error of the number of fitted values for each subset regression model, and best model selection is done based on the smallest Cp-value. The results of the analysis are summarized in Table 4.13. Best subset model process selects the best model according to these criteria for a model of a particular size. If the predictor is selected to be in the model, it is rated as 1 or "True", and if not 0 or "False".

Table 4.13 Best subset model selection output

M	#	Int.	ω_{opt}	γ_{dry}	Percent Fines	R-value	Grading	Adj. R^2	C_p	AIC	BIC
1	1	1	0	0	0	0	1	0.323	10.399	190.732	191.528
2	1	1	1	0	0	0	0	0.097	16.196	193.895	194.691
3	1	1	0	0	0	1	0	0.085	16.522	194.049	194.845
4	2	1	0	1	0	0	1	0.516	6.053	187.742	188.935
5	2	1	0	0	0	1	1	0.356	9.705	190.882	192.076
6	2	1	1	0	0	0	1	0.283	11.387	192.073	193.267
7	3*	1	0	1	0	1	1	0.669	3.625	184.110	185.702
8	3	1	1	1	0	0	1	0.495	7.085	188.734	190.325
9	3	1	0	1	1	0	1	0.472	7.550	189.229	190.821
10	4$	1	1	1	0	1	1	0.702	4.101	183.236	185.225
11	4	1	0	1	1	1	1	0.626	5.413	185.754	187.744
12	4	1	1	1	1	0	1	0.433	8.709	190.316	192.305
13	5	1	1	1	1	1	1	0.650	6.000	185.015	187.403

M−Subset model, #−Number of predictors, Int.−Intercept, 0−False, 1−True, Adj. R^2 –adjusted R-square, *−Best model based on the smallest C_p value, $−Best model based on the largest adjusted R^2 value and the smallest AIC and BIC values.

The best subset model No. 10 based on the highest adjusted R-square value and the smallest AIC and BIC values has four terms. However, based on the smallest Cp criterion, the subset model No. 7 with three terms is the best subset model. This best subset model No. 7 based on the Cp criterion agrees with the model given by Equation (4.1) which was developed by the elimination of non-significant predictors at a significance level of 0.1. The alternative prediction model No. 10 is given by

$$\widehat{M}_r = 296865.8 - 4562.5(\omega_{opt}) - 1992.6(\gamma_{dry}) + 612.3(R) - 10388.3(Grading) \quad (4.2)$$

where,

$\widehat{M}_r$= estimated resilient modulus at optimum moisture content (psi),
ω_{opt} = optimum moisture content (percentage),
γ_{dry} = maximum dry density (pcf),
R = R-value determined from T-190 test at 300 psi exudation pressure, and
Grading = “1” for W-grading and “0” for L-grading.

4.7.2.1 Assessment of Models

Assumptions on the model errors should be checked before applying a model. This includes checking consistency, normality, lack of fit, and independence of model errors. The residuals indicate that the model errors (t-statistics and p-value) were consistent and normal. The Breush-Pagan and Shapiro Wilk test results of the two models are summarized in Table 4.14.

Table 4.14 Consistency and normality test results for the two estimation models

Estimation Model	p-value for Consistency (Breush-Pagan Test)	p-value for Normality (Shapiro Wilk Test)
Equation (4.1)	0.24	0.77
Equation (4.2)	0.15	0.24

Since the p-value obtained from both the Breush-Pagan test and the Shapiro-Wilk test were greater than the 0.1 significance level, the consistency and normality of both models were satisfied. Therefore, the best prediction model was selected by ranking the predicted models according the selection criteria, and the best model is Equation (4.2) with the error sum of squares of 76,027,272 and adjusted R-square of 0.70. The regression coefficients of the Equation (4.2) are summarized in Table 4.15.

Table 4.15 Summary of regression coefficients for Equation (4.2)

Statistical Predictors	Estimates	Std. Error	t-value	p-value
Intercept	296865.8	91010.2	3.262	0.0172
ω_{opt}	-4562.5	3408.5	-1.339	0.2292
γ_{dry}	-1992.6	643.2	-3.098	0.0212
R value	612.3	252.9	2.421	0.0518
Grading	-10388.3	3014.4	-3.446	0.0137

Plotting the estimated M_r value using Equation (4.2) to the laboratory-measured M_r values in Figure 4.16, the predicted model was found to have 82 percent of the variability in laboratory measured M_r value.

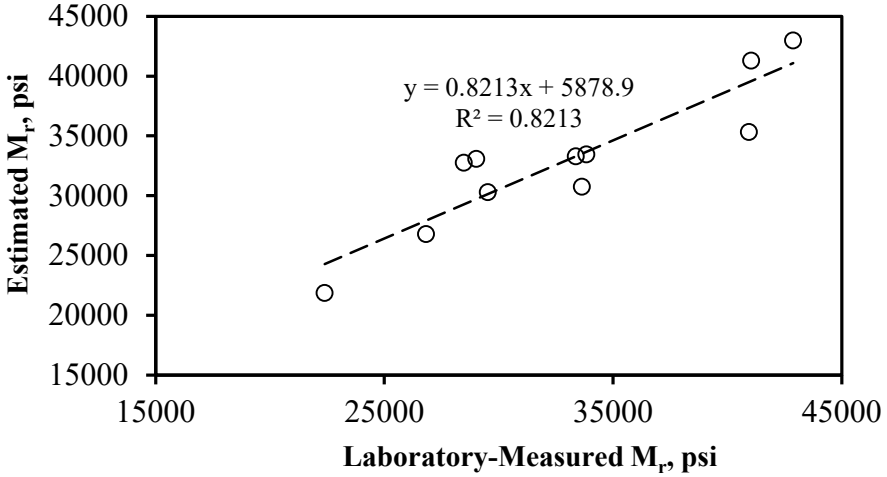

Figure 4.16 Comparison of predicted M_r using Equation (4.2) to the laboratory-measured M_r

4.8 Constitutive Models

The commonly used nonlinear constitutive models discussed in Section 2.8 were calibrated in this section. Both linear and nonlinear regression methods were used to determine the regression coefficients of these models for test samples at optimum moisture content. Also, one representative regression coefficient for A-1-a soil type was determined in according with the AASHTO M 145 (1991). The error sum of squares (SSE) was used to compare the results of linear and nonlinear regression coefficients. The constitutive regression coefficients were denoted as K_1, K_2, and K_3 for the Equation (2.7) and K_1 and K_2 for the Equation (2.3). Both the linear and nonlinear analyses were performed for the 11 aggregates at optimum moisture content as summarized in Table 4.16, for the Hicks and Monismith (1971) model, and Table 4.17 for the NCHRP (2004) model. The average M_r values at optimum moisture content from Table 4.3 of each load sequence were taken in computing the constitutive coefficients. The average representative M_r values, bulk stresses, and octahedral stresses computed from the laboratory measured data are summarized in Table 4.18. Tables 4.17 and 4.18 show that the nonlinear regression model provides smaller error sum of squares (SSE) than the linear regression analysis. Hence, the final constitutive coefficients were computed using the nonlinear regression analysis.

The bulk stress was computed by adding the axial stress and two times the confining stress. The octahedral stress was found by multiplying the deviatoric stress by $\sqrt{2}/3$ and the deviator stress, which is determined by subtracting the confining stress from the axial stress. Finally, the average M_r of each load sequence for the 11 samples tested at optimum moisture content was prepared to represent the soil classified as A-1-a, and the results are summarized in Table 4.18. The constitutive coefficients using the nonlinear regression analysis of Equation (2.3) and Equation (2.7) were computed and summarized in Table 4.19.

Table 4.16 Regression coefficients of Hicks and Monismith (1971) model

Linear regression model: $\log_{10} M_r = \log_{10} K_1 + K_2 \log_{10} \theta + \varepsilon$				**Non-linear regression model:** $M_r = K_1 \theta^{K_2} + \varepsilon$		
AGG. #	**K_1**	**K_2**	**SSE**	**K_1**	**K_2**	**SSE**
4	1,527.658	0.752	19,279,205	1,708	0.720	17,487,916
5	2,902.043	0.648	49,105,485	3,368	0.610	43,240,875
6	2,704.647	0.662	28,252,476	2,962	0.640	26,267,568
7	2,179.014	0.705	42,740,990	2,488	0.670	38,982,570
8	4,830.875	0.603	215,247,135	5,981	0.550	189,941,914
9	5,228.117	0.594	161,007,045	6,264	0.550	141,032,065
10	2,984.557	0.645	40,439,442	3,474	0.600	33,947,946
11	3,879.223	0.609	69,574,551	4,583	0.560	59,174,500
12	3,731.734	0.673	176,315,800	4,518	0.620	158,018,172
13	2,366.444	0.742	119,509,409	3,264	0.660	82,688,135
14	2,904.815	0.678	66,016,179	3,526	0.630	55,657,954

AGG. #−Aggregate No., $K_{1,}$ $K_{2,\ and}$ K_3 –Regression coefficients, θ–Bulk stress, SSE–Sum of square errors, and ε–Error.

Table 4.17 Regression coefficients of NCHRP (2004) model

Linear regression model: $\log_{10}\left(\frac{M_r}{p_a}\right) = \log_{10} K_1 + K_2 \log_{10}\left(\frac{\theta}{p_a}\right) + K_3 \log_{10}\left(\frac{\tau_{oct}}{p_a}+1\right) + \varepsilon$					**Non-linear regression model:** $M_r = K_1 p_a \left(\frac{\theta}{p_a}\right)^{K_2} \left(\frac{\tau_{oct}}{p_a}+1\right)^{K_3} + \varepsilon$			
AGG. #	**K_1**	**K_2**	**K_3**	**SSE**	**K_1**	**K_2**	**K_3**	**SSE**
4	790.6526	0.7657	-0.103	10,375,542	808.74214	0.76267	-0.19566	7,074,919
5	1152.7012	0.6859	-0.2833	14,190,580	1182.4464	0.65722	-0.26874	11,651,361
6	1110.8039	0.693	-0.2314	8,739,628	1123.6651	0.67656	-0.20681	8,002,173
7	1008.9781	0.7449	-0.3021	9,471,681	1026.7534	0.72292	-0.28108	8,298,339
8	1712.7628	0.6525	-0.368	86,918,187	1786.6727	0.61025	-0.36979	73,676,664
9	1795.7522	0.6326	-0.2907	71,933,842	1862.2256	0.59663	-0.29472	61,059,450
10	1170.284	0.6737	-0.2118	16,092,819	1205.85	0.64444	-0.2177	12,618,268
11	1384.8997	0.6431	-0.2531	27,953,211	1431.6624	0.60948	-0.25432	22,269,914
12	1595.6243	0.7224	-0.37	74,496,940	1649.3575	0.68113	-0.32421	65,071,403
13	1207.9348	0.7771	-0.2629	59,927,659	1297.993	0.70891	-0.28136	35,553,887
14	1241.5543	0.7016	-0.1803	33,836,238	1295.6403	0.67141	-0.22992	26,612,328

AGG. #−Aggregate No., K_1, K_2, and K_3–Regression coefficients, θ–Bulk stress, τ_{oct}−Octahedral shear stress, SSE–Error Sum of squares, and ε–Error.

Table 4.18 Average M_r, bulk stress, and octahedral stress at optimum moisture content

Load Sequence	**M_r, psi**	**Bulk stress (θ), psi**	**Octahedral stress (τ_{oct}), psi**
1	13126.8	9	0
2	15814	12	1.414
3	18233.64	15	2.828
4	18783	15	0
5	22898.09	20	2.357
6	26149.27	25	4.714
7	32214.18	30	0
8	36869.27	40	4.714
9	38825.64	50	9.428
10	38408.73	40	2.357
11	40257.45	45	0
12	44576.64	60	7.071
13	46514.18	55	2.357
14	48308.36	60	0
15	50733.55	80	9.428

Table 4.19. Base layer constitutive coefficients.

Statistical Parameter	NCHRP (2004) model				Hicks and Monismith (1971) model		
	K_1	K_2	K_3	SSE	K_1	K_2	SSE
Estimate	1332.978	0.660	-0.272	18,678,830	3775.0	0.610	60,077,073
Std. Error	32.1966	0.0217	0.0527		481.9	0.0331	
t value	41.401	30.427	-5.164		7.834	18.438	
P-value	2.55E-14	9.96E-13	2.36E-04		2.81E-06	1.06E-10	

SSE–Error Sum of squares.

The locally calibrated NCHRP (2004) prediction model and the Hicks and Monismith (1971) model are given by Equation (4.3) and Equation (4.4), respectively.

$$\widehat{M}_r = 1332.978 P_a \left(\frac{\theta}{P_a}\right)^{0.66} \left(\frac{\tau_{oct}}{P_a} + 1\right)^{-0.272} \quad (4.3)$$

$$\widehat{M}_r = 3775(\theta)^{0.61} \quad (4.4)$$

where,

θ = bulk stress = $\sigma_1 + \sigma_2 + \sigma_3 = \sigma_1 + 2\sigma_3$ (psi),
σ_1 = axial stress (psi),
$\sigma_2 = \sigma_3$ = confining stress (psi)
$\sigma_d = \sigma_1 - \sigma_3$= deviator stress (psi),
τ_{oct} = octahedral shear stress = $\frac{1}{3}\sqrt{(\sigma_1 - \sigma_2)^2 + (\sigma_1 - \sigma_3)^2 + (\sigma_2 - \sigma_3)^2}$ (psi), and
P_a = atmospheric condition or unit reference pressure equal to 14.7 psi (101.3 kPa).

The comparison between laboratory measured and predicted resilient moduli based on Equations (4.3) and (4.4) are plotted in Figure 4.17 and Figure 4.18, respectively. The results show a very good fit with respective R-square values of 0.99 and 0.98.

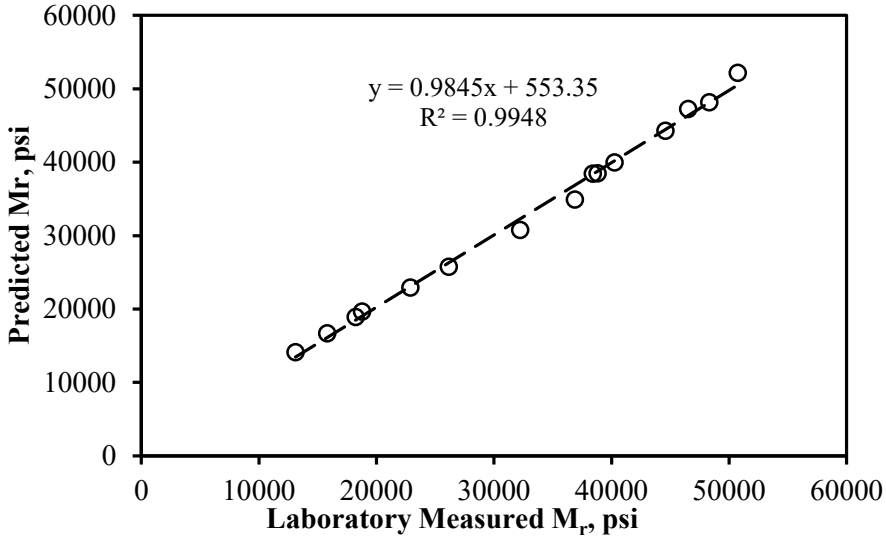

Figure 4.17 Comparison of predicted M_r using the NCHRP (2004) model and the laboratory-measured M_r

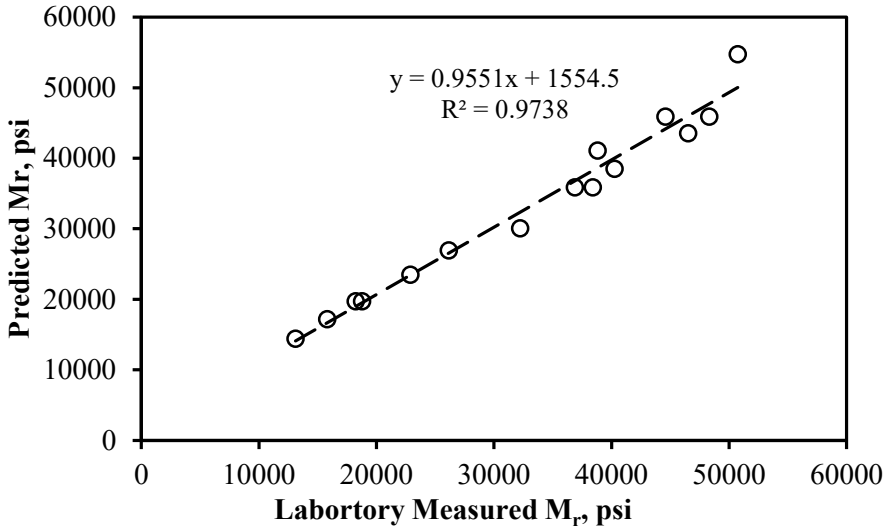

Figure 4.18 Comparison of predicted M_r using the Hicks and Monismith (1971) model and laboratory-measured M_r

4.9 Design Chart

Since laboratory determination of resilient modulus is tedious and time consuming, a design chart developed from laboratory measured resilient modulus will facilitate the implementation of MEPDG in Wyoming. Design of pavement using the AASHTOWare ME- software is an iteration process that constantly changes the thicknesses of the surface layer and base layer until all the payment distresses and performance limits are below critical values. In this study, typical dry unit weight, Poisson's ratio, and elastic modulus of asphalt material as well as tire pressure and contact radius are summarized in Table 4.20 based on the recommendations by Henrichs (2015).

Table 4.20 Assumed typical asphalt properties, and tire pressure and radius

Material	Dry Unit Weight (pcf)	Elastic Modulus (psi)	Poisson's ratio	Tire pressure (psi)	Contact radius (in)
Asphalt	145	500,000	0.5	100	5

The deviator stress was computed at the top of base layer using KENPAV computer package for pavement analysis and design at a tire pressure of 100 psi (689.47 kPa) to simulate the trucks tire pressure in Wyoming for assumed hot mix asphalt thicknesses of 4, 6, 8, 10, and 12 inches. The hot mix asphalt is assumed as linear elastic, bonded layer interface with base layer, and one layer for top compression and bottom tension of asphalt thickness. The load group is assumed as single axle with single tire. The KENPAV output results are displayed in the thesis by Mebrahtom (2017). The confining stress is calculated by Equation (4.5).

$$\sigma_c = K_0(\gamma_{dry} \times Z + \sigma_d) \quad (4.5)$$

where,

σ_c = confining stress (psi),
K_0 = coefficient of later earth pressure (assumed as 0.5),
γ_{dry} = dry unit weight (psi),
Z = hot mix asphalt thickness (inch), and
σ_d = vertical stress on the top the base layer (psi).

The computed deviator stress, confining stress, and bulk stress are summarized in Table 4.21. Finally, the computed bulk stress ($i.e., \theta = \sigma_d + 3 \times \sigma_c$) was rounded up to nearest laboratory bulk stress to minimize the interpolation or extrapolation errors. The resilient modulus at optimum moisture content for A-1-a soil was taken from the corresponding bulk stress summarized in Table 4.18.

Table 4.21 Summary of deviator and confining stresses at top of a base layer for assumed pavement design thicknesses

Stress and M_r	**Asphalt Thickness (inch)**				
	4	6	8	10	12
Deviator stress, psi	29.3	15.6	10.0	6.8	5.0
Confining stress, psi	14.8	8.1	5.3	3.8	3.0
Bulk stress, psi	73.8	39.8	25.9	18.4	13.9
Rounded up bulk stress, psi	80	40	30	20	15
Corresponding M_r, psi	50734	38826	26149	22898	18783

The design chart shown in Figure 4.19 was developed using the data summarized in Table 4.21. The estimated resilient modulus taken from this design chart is only applicable for A-l-a untreated base materials at optimum moisture content.

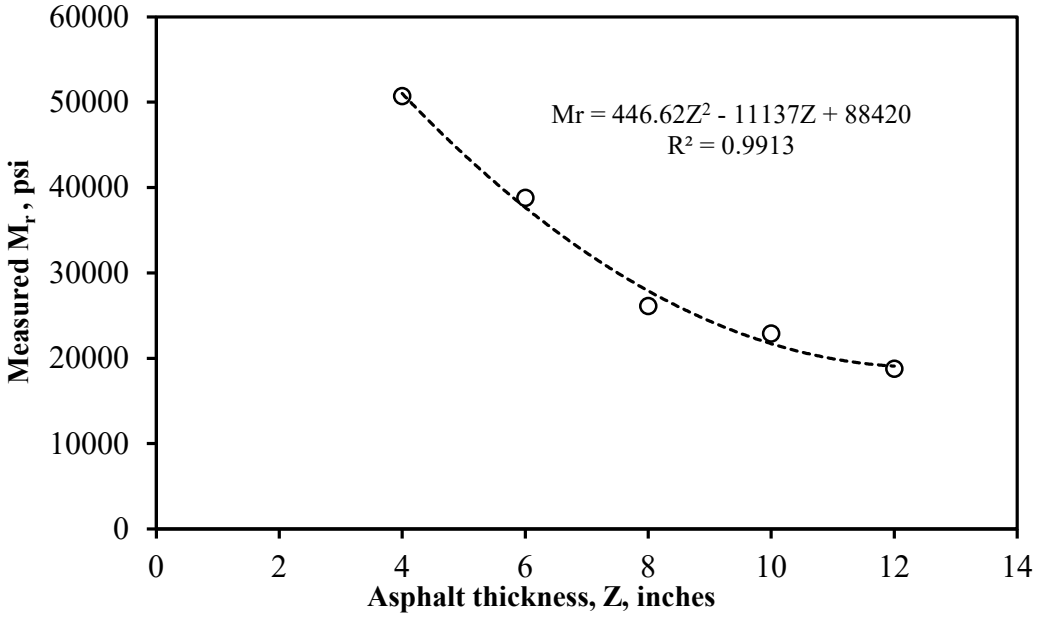

Figure 4.19 Design chart of measured resilient modulus as a function of asphalt thickness

For Level -3 inputs, laboratory derived resilient modulus, R-value, maximum dry density, optimum moisture content, percent fines and the current Level-3 default resilient modulus obtained from the design software AASHTOWare® are summarized in Table 4.22. The default Level-3 resilient modulus given in AASHTOWare® is higher than the WYDOT mean resilient modulus. The R-value and maximum dry density of the Wyoming base materials are greater than the default values even though the default optimum moisture content of 7.4 percent is about 13.85 percent higher than the mean optimum moisture content of local base materials.

Table 4.22 Summary of laboratory derived M_r value and other typical properties of A-1-a base material

AASHTO Soil Class	Statistical Parameter/ Default	M_r value, psi	R-value	γ_{dry}, pcf	ω_{opt} (percent)	Percent Fines
A-1-a	Mean	32,906	80	138.3	6.5	8.5
	Std. Dev	6,523.5	4.6	2.03	0.36	2.07
	Min.	22,388	75	135.4	6.2	5.9
	Max.	42,878	88	141.5	7.2	11.9
	Default	40,000	72	127.2	7.4	8.7

Std. Dev−Standard deviation, Min.−Minimum, Max.−Maximum, ω_{opt}–optimum moisture content, and γ_{dry}–Maximum Dry Density.

5. SUMMARY, CONCLUSIONS, AND RECOMMENDATIONS

5.1 Summary

In this study, a laboratory resilient modulus testing was conducted using a wide range of base materials located in Wyoming. The characteristics and index properties of these base materials selected for testing were determined. Statistical analysis was conducted to determine two local empirical models for M_r. These empirical models enable WYDOT engineers to estimate the resilient modulus of the base materials for future pavement design without the need to conduct laboratory resilient modulus testing. Constitutive coefficients were locally calibrated for the NCHRPR (2004) model and the Hicks and Monismith (1971) model using the nonlinear regression analysis. The constitutive coefficients determined at optimum moisture content are helpful in computing the resilient modulus of the base layer for a known bulk stress and octahedral shear stress, which are dependent on the wheel load and hot mix asphalt (HMA) thickness. Finally, a design table and a design chart for resilient modulus were developed to facilitate the design process. The current Level-3 MEPDG properties were compared with the locally measured resilient modulus. The outcomes of this research will facilitate the implementation of MEPDG in Wyoming.

5.2 Conclusions

The results from this study are intended for the roadway conditions, base materials, and construction practices in Wyoming, but the methodology of testing and statistical analysis can be adopted by other Departments of Transportation. The following conclusions are drawn from this study:

(1) The resilient modulus of base material increases with increasing confining stress at both low and high bulk stress levels. Considering bulk stress in the estimation of M_r is the correct approach in this study.
(2) The resilient modulus of the base materials was found to be decreasing with increasing moisture content.
(3) Due to a narrow range of percent fines between 5.9 and 11.9 percent of the base materials used in this study, the influence of percent fines on resilient modulus was not significant.
(4) The R-value of the L-grading base materials was found to be higher than that of the W-grading.
(5) In this study, aggregate gradation was found to be highly significant in estimating the resilient modulus. Based on the test results and prediction models developed from this study, the L-grading samples were found to have a higher M_r value than the W-grading.
(6) A model was developed to predict base resilient modulus based on standard base properties (i.e., R-value, maximum dry density, optimum moisture content, and grading). This model is beneficial when it is desirable to estimate the resilient modulus without performing the expensive and time consuming resilient modulus test.

5.3 Recommendations

The following recommendations are provided to facilitate the implementation of MEPDG. However, it is important to note that all regression models developed in this study should be only applicable to untreated base materials.

(1) The resilient modulus, in terms of the influential predictors, can be estimated by Equation (4.1) and Equation (4.2). Because this model yields lower error sum of squares, Equation (4.2) is the most preferable model in the estimation of the resilient modulus,

$$\widehat{M}_r = 296865.8 - 4562.5(\omega_{opt}) - 1992.6(\gamma_{dry}) + 612.3(R) - 10388.3(Grading)$$

where,

$\widehat{M}_r$= estimated resilient modulus at optimum moisture content (psi),
ω_{opt} = Optimum moisture content (percentage),
γ_{dry} = maximum dry density (pcf),
R = R-value determined from T-190 test at 300 psi exudation pressure, and
Grading = "1" for W-grading and "0" for L-grading.

(2) The calibrated NCHRP (2004) and Hicks and Monismith (1971) constitutive models for the A-1-a soil classification are given by Equation (4.3) and Equation (4.4), respectively. The calibrated NCHRP (2004) constitutive model given by Equation (4.4) yields lower error sum of squares, and hence, this model is recommended;

$$\widehat{M}_r = 1332.978 P_a \left(\frac{\theta}{P_a}\right)^{0.66} \left(\frac{\tau_{oct}}{P_a} + 1\right)^{-0.272}$$

where,

$\theta = \text{bulk stress} = \sigma_1 + \sigma_2 + \sigma_3 = \sigma_1 + 2\sigma_3$ (psi),
σ_1 = axial stress (psi),
$\sigma_2 = \sigma_3$ = confining stress (psi)
$\sigma_d = \sigma_1 - \sigma_3$= deviator stress (psi),
$\tau_{oct} = \text{octahedral shear stress} = \frac{1}{3}\sqrt{(\sigma_1 - \sigma_2)^2 + (\sigma_1 - \sigma_3)^2 + (\sigma_2 - \sigma_3)^2}$ (psi), and
P_a = atmospheric condition or unit reference pressure equal to 14.7 psi (101.3 kPa).

(3) The design chart shown in Figure 4.19 can be used for the estimation of M_r values when the hot mix asphalt thickness is known.
(4) If only known characteristic of the crushed aggregate is soil classification, the resilient modulus along with other standard base properties summarized in Table 4.22 can be used as the defaulted Level-3 inputs for pavement designs in Wyoming.
(5) If additional base testing is conducted by WYDOT in the future, the M_r models developed in this study should be recalibrated to include new test data.
(6) A similar study should be conducted to characterize the treated base materials.
(7) The AASHTO MEPDG user's guide (2012) currently used by WYDOT shall be updated to incorporate new findings from this study.

REFERENCES

American Association of State Highway and Transportation Officials (AASHTO), T 292, 1991. Interim Method of Test for Resilient Modulus of Subgrade Soils and Untreated Base/Subbase Materials. Washington, D.C.

American Association of State Highway and Transportation Officials (AASHTO) M 145, 1991. Standard Specification for Classification of Soils and Soil-Aggregate Mixtures for Highway Construction Purposes. Washington, D.C.

American Association of State Highway and Transportation Officials (AASHTO) T 294, 1992. Standard Method of Test for Resilient Modulus of Unbound Granular base/Subbase Materials and Subgrade Soil-SHRP Protocol P46. Washington, D.C.

American Association of State Highway and Transportation Officials (AASHTO), 1993. AASHTO Guide for Design of Pavement Structures, Vol. 1, Washington, D.C.

American Association of State Highway and Transportation Officials (AASHTO) TP 46, 1994. Standard Method of Test for Determining the Resilient Modulus of Soils and Aggregate Materials. Washington, D.C.

American Association of State Highway and Transportation Officials (AASHTO) TP 31, 1996. Standard Method of Test for Determining the Resilient Modulus of Bituminous Mixtures by Indirect Tension. Washington, D.C.

American Association of State Highway and Transportation Officials (AASHTO) T 307, 2007. Standard Method of Test for Determining the Resilient Modulus of Soils and Aggregate Materials. Washington, D.C.

American Association of State Highway and Transportation Officials (AASHTO) T 99, 2010. Standard Method of Test for Moisture-Density Relations of Soils Using a 5.5-lb Rammer and a 12-in Drop. Washington, D.C.

American Association of State Highway and Transportation Officials (AASHTO) T 180, 2015. Standard Method of Test for Moisture-Density Relations of Soils Using a 10-lb Rammer and a 18-in Drop. Washington, D.C.

Allen, J.J. and Thompson, M.R., 1974. Resilient Response of Granular Materials Subjected to Time Dependent Lateral Stresses. Journal of the Transportation Research Record, No. 510, Transportation Research Board, pp. 1-13. (http://worldcat.org/issn/03611981)

Allen, J.J., 1973. The Effect of Non-Constant Lateral Pressures of the Resilient Response of Granular Materials. Doctoral dissertation, University of Illinois at Urbana-Champaign, Urbana, IL.

Andrei, D.E., 2004. Harmonized Resilient Modulus Test Method for Unbound Pavement Materials. Journal of the Transportation Research Record, No. 1874, Transportation Research Board, pp. 29-37. (https://doi.org/10.3141/1874-04)

Pappin, J.W., 1979. Characteristics of Granular Material for Pavement Analysis. Doctoral dissertation, University of Nottingham, Department of Civil Engineering, Nottingham, England.

Barksdale, R.D and Itani S.Y., 1989. Influence of Aggregate Shape on Base Behavior. Journal of the Transportation Research Record, No. 1227, Transportation Research Board, pp. 173-182. (http://worldcat.org/isbn/0309048222)

Brown, S.F and Hyde, A., 1975. Significance of Cyclic Confining Stress in Repeated-Load Traixial Testing of Granular Material. Journal of the Transportation Research Record, No. 537, Transportation Research Board, pp. 49-58. (http://worldcat.org/isbn/0309023882)

Brown, S.F. and Selig, E.T., 1991. The Design of Pavement and Rail Track Foundations. In the Proceedings of cyclic loading of soils: From theory to design. M.P. O'Reilly and S.F. Brown, eds. Blackie and Son Ltd, Glasgow, Scotland.

Cary, C.E. and Zapata, C.E., 2011. Resilient Modulus for Unsaturated Unbound Materials. Journal of Road Materials and Pavement Design, 12(3), pp. 615-638. (http://www.tandfonline.com/doi/abs/10.1080/14680629.2011.9695263)

Haynes, J. G. and Yoder, E.J., 1963. Effects of Repeated Loading on Gravel and Crushed Stone Base Course Materials Used in the AASHO Road Test. FHWA/IN/JHRP-63/04. Joint Highway Research Project, Indiana Department of Transportation and Purdue University, West Lafayette, IN.

(http://docs.lib.purdue.edu/cgi/viewcontent.cgi?article=1970&context=jtrp)

Hellrung, D., 2015. Back-Calculation on the Subgrade Resilient Modulus for Mechanistic-Empirical Pavement Design in Wyoming. Master Thesis, University of Wyoming, Department of Civil and Architectural Engineering, Laramie, WY.

Henrichs, Z.R., 2015. Measurement of The Resilient Modulus of Subgrade Materials for Mechanistic-Empirical Pavement Design Guide in Wyoming. Masters Thesis, University of Wyoming, Department of Civil and Architectural Engineering, Laramie, WY.

Heydinger, A.G., 1996. Analysis of Resilient Modulus of Dense and Open-Graded Aggregates. Journal of the Transportation Research Record, No. 1547, Transportation Research Board, pp. 1–6. (https://doi.org/10.3141/1547-01)

Hicks, R.G., 1970. Factors Influencing the Resilient Properties of Granular Materials. Doctoral dissertation, University of California, Berkeley, CA.

Hicks, R.G. and Monismith, C.L., 1971. Factors Influencing the Resilient Properties of Granular Materials. Highway Research Record 345, pp.15–31. (https://trid.trb.org/view.aspx?id=104720)

Hossain, M.S. and Lane, D.S., 2015. Development of a Catalog of Resilient Modulus Values for Aggregate Base for Use With the MechanisticEmpirical Pavement Design Guide (MEPDG). Final Report VCTIR 15-R13, Virginia Transportation Research Rouncil, Charlottesville, VA. (http://vtrc.virginiadot.org/PubDetails.aspx?id=298224)

Huang, Y. H., 1993. Pavement Analysis and Design. 2nd Edition, Pearson Prentice Hall, NJ. (https://drive.google.com/file/d/0B6ehKjDUHJiGMzNtNjFxT1U0cm8/view)

Jorenby, B.N. and Hicks, R.G., 1986. Base Course Contamination Limits. Journal of the Transportation Research Record, No. 1095, Transportation Research Board, pp. 86-101. (http://worldcat.org/isbn/0309041155)

Kancherla, A., 2004. Resilient Modulus and Permanent Deformation Testing of Unbound Granular Materials. Master Thesis, Texas A&M University, College Station, TX. (http://oaktrust.library.tamu.edu/bitstream/handle/1969.1/2711/etd-tamu-2004B-CVEN-Kancherla.pdf?sequence=1)

Kolisoja, P., 1997. Resilient Deformation Characteristics of Granular Materials. Doctoral dissertation, Tampere University of Technology, publ. No. 223, Tampere, Finland.

Lekarp, F, Isacsson, U., and Dawson, A., 2000. State of the Art. I: Resilient Response of Unbound Aggregates. Journal Transportation Engineering, 126(1), pp. 66-75. (https://doi.org/10.1061/(ASCE)0733-947X(2000)126:1(66))

Mebrahtom, D, 2017. Characterization of Crushed Base Materials in Wyoming. Master Thesis, University of Wyoming, Department of Civil and Architecural Engineering, Laramie, WY.

Mishra, D.T., 2010. Quantifying Effects of Particle Shape and Type and Amount of Fines on Unbound Aggregate Performance through Controlled Gradation. Journal of the Transportation Research Record, No. 2167, Transportation Research Board, pp. 61-71. (https://doi.org/10.3141/2167-07)

Mitry, F.G., 1965. Determination of the Modulus of Resilient Deformation of Untreated Base Course Materials. Doctoral dissertation, University of California, Berkeley, CA.

Monismith, C.L., Seed, H.B., Mitry, F.G., and Chan, C.K., 1967. Prediction of Pavement Deflections from Laboratory Tests. In the Proceedings of 2nd International Conference on the Structural Design of Asphalt Pavements, Ann Arbor, MI, pp. 109-140. (https://trid.trb.org/view.aspx?id=717129)

National Cooperative Highway Research Program (NCHRP), 2004. Guide for Mechanistic-Empirical Design of New and Rehabilitated Pavement Structures. NCHRP Report 01-37A. Transportation Research Board, National Research Council, Washington, D.C.

National Cooperative Highway Research Program (NCHRP), 2004. Laboratory Determination of Resilient Modulus for Flexible Pavement Design. NCHRP Report 01-28A. Transportation Research Board, National Research Council, Washington, D.C.

Ng, K.W., Hutson, Z., Ksaibati, K., and Wulff, S. S., 2017. A Comprehensive Field and Laboratory Test Programme and Electronic Database of Pavement Material Properties for MEPDG. International Journal of Pavement Engineering, pp. 1-15. (http://dx.doi.org/10.1080/10298436.2017.1316846)

Puppala, A.J., 2008. Estimating Stiffness of Subgrade and Unbound Materials for Pavement Design. A Synthesis of Highway Practice, NCHRP Synthesis 382, Transportation Research Board, Washington D.C. (http://www.trb.org/Main/Public/Blurbs/160578.aspx)

Raad, L.M., 1992. Characterization of Saturated Granular Bases under Repeated Loads. Journal of the Transportation Research Record, No. 1369, Transportation Research Board, pp. 73-82. (http://worldcat.org/isbn/0309054109)

Richard Ji, Siddiki, N., Natung, T., and Kim, D., 2014. Evaluation of Resilient Modulus of Subgrade and Base Materials in Indiana and its Implementation in MEPDG. The Scientific World Journal, Vol. 2014, pp. 1-15. (http://dx.doi.org/10.1155/2014/372838)

Seed, H.B., Mitry, F.G., Monismith, C.L., and Chan, C.K., 1967. Prediction of Flexible Pavement Deflections from Laboratory Repeated Load Tests. NCHRP Report No. 35, National Cooperative Highway Research Program, Transportation Research Board, Washington, D.C. (http://worldcat.org/issn/00775614)

Smith, W.S. and Nair, K., 1973. Development of Procedures for Characterization of Untreated Granular Base Course and Asphalt-Treated Base Course Materials. FHWA-RD-74-61, Federal Highway Administration, U.S. Department of Transportation, Washington, D.C. (https://archive.org/details/developmentofpro00mate)

Sweere, G.T.H., 1990. Unbound Granular Bases for Roads . Doctoral dissertation, Delft University of Technology, Netherlands. (http://www.citg.tudelft.nl/fileadmin/Faculteit/CiTG/Over_de_faculteit/Afdelingen/Afdeling_Bouw/-_Secties/Sectie_Weg_en_Railbouwkunde/-_Leerstoelen/Leerstoel_Wegbouwkunde/-_Publicaties/-_Proefschriften/doc/Sweere_-_Dissertation_Sweere.pdf)

Thom, N. H., 1988. Design of Road Foundations. Doctoral dissertation, Department of Civil Engineering, University of Nottingham, Nottingham, England. (http://eprints.nottingham.ac.uk/10281/)

Thom, N.H. and Brown, S.F., 1988. The Effect of Grading and Density on the Mechanical Properties of a Crushed Dolomitic Limestone. In the Proceedings of the 14th Austrlian Road Research Board (ARRB) Conference, Vol. 14, Issue 7, Canberra, Australia, pp. 94–100. (http://arrbknowledge.com)

Tian, P., Zaman, M., and Laguros, J., 2014. Gradation and Moisture Effects on Resilient Moduli of Aggregate Bases. Journal of the Transportation Research Record, No. 1619, Transportation Research Board, pp. 75-84.

(http://trrjournalonline.trb.org/doi/abs/10.3141/1619-09)

Uzan, J., 1985. Characterization of Granular Materias. Journal of the Transportation Research Record, No. 1022, Transportation Research Board, pp.52-59. (http://worldcat.org/isbn/0309039118)

Uzan, J., 1992. Resilient Characterization of Pavement Materials. International Journal for Numerical and Analytical Methods in Geomechanics, 16(6), pp. 453-459. (http://onlinelibrary.wiley.com/doi/10.1002/nag.1610160605/abstract)

Vuong, B., 1992. Influence of Density and Moisture Content on Dynamic Stress-Strain Behaviour of a Low Plasticity Crushed Rock. Road and Transport Research, 1(2), pp. 88-100. (http://worldcat.org/oclc/26087078)

Wyoming Department of Transportation (WYDOT) (2017). *Standard Specifications for Road and Bridge Construction*. Cheyenne, WY. (ftp://wydot-filestore.dot.state.wy.us/construction/constructionmanuals/2017%20Construction%20Manual/)